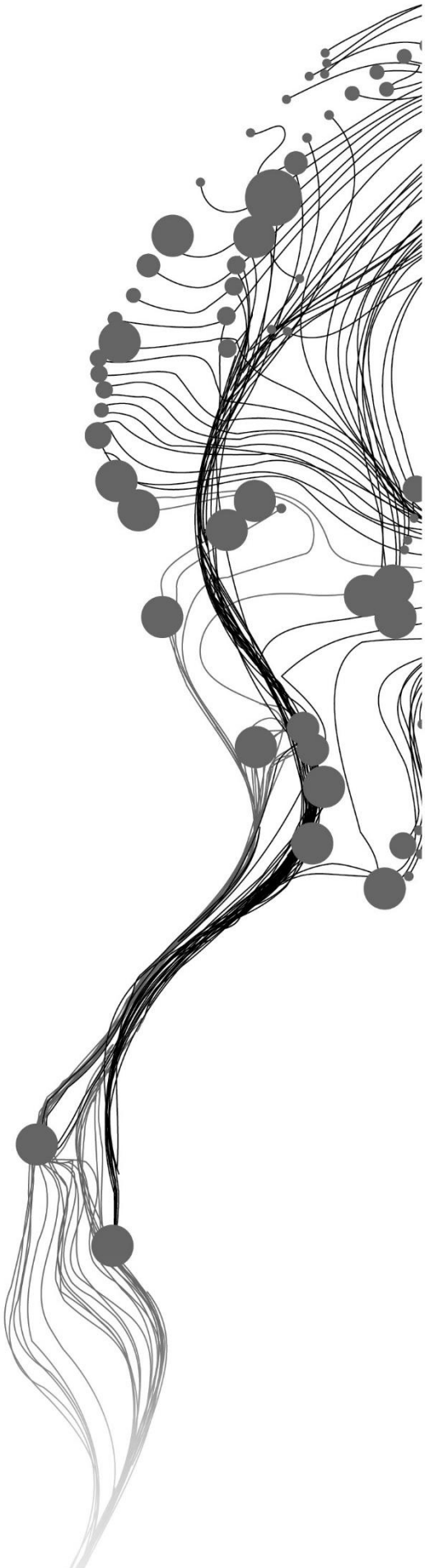

OPTIMIZATION OF UAV FLIGHT PLANS IN DIFFICULT LANDSCAPES

ZIYAO WANG

June, 2020

SUPERVISORS:
Dr. F.C. Nex
Dr. V.V. Lehtola

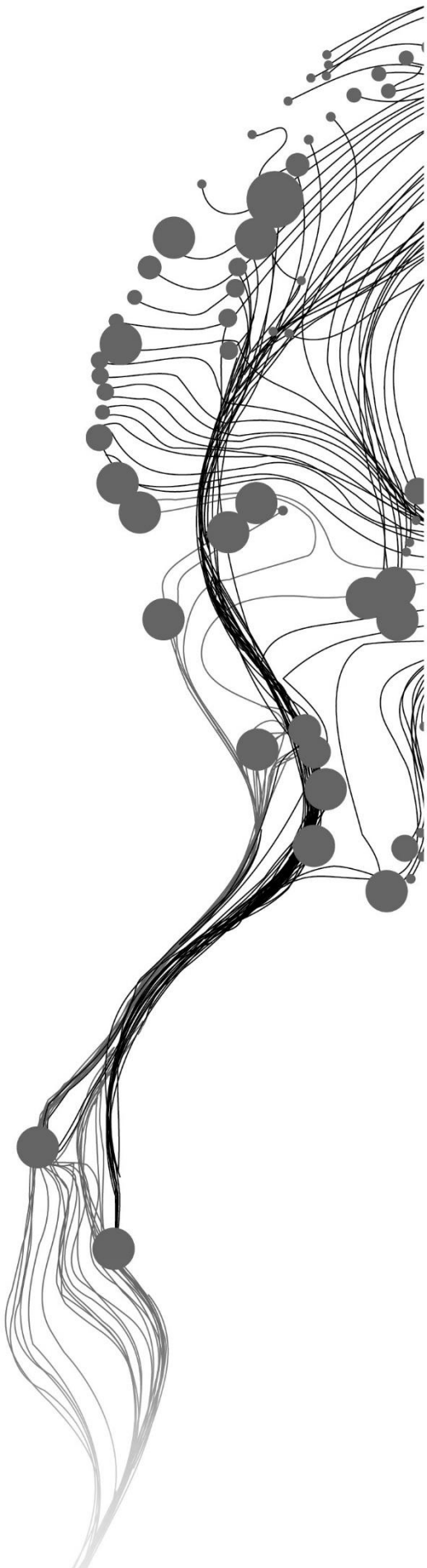

Optimization of UAV flight plans in difficult landscapes

ZIYAO WANG
Enschede, The Netherlands, June, 2020

Thesis submitted to the Faculty of Geo-Information Science and Earth Observation of the University of Twente in partial fulfilment of the requirements for the degree of Master of Science in Geo-information Science and Earth Observation.
Specialization: Geoinformatics

SUPERVISORS:
Dr. F.C. Nex
Dr. V.V. Lehtola

THESIS ASSESSMENT BOARD:
Prof.Dr.ir. M.G. Vosselman (Chair)
Dr. F. Remondino (External member, Bruno Kessler Foundation, 3DOM research unit, Italy)

ABSTRACT

With the continuous progress and development of technology, Unmanned Aerial Vehicle (UAV) have been widely used in the field of surveying and mapping. UAV is able to collect high-resolution, close-range photogrammetry data at a low cost, and the flexibility of the UAV allows it to customize the carried sensors according to the mission requirements. However, due to the limitation of UAV flight height, there is often insufficient coverage when performing photogrammetry mission in undulating terrain as mountainous areas, which affects quality of data set. In order to avoid insufficient coverage, the commonly used method in actual flight is to set the image overlap much higher than required, which means that the distribution of viewpoints will be denser, further causing data redundancy. In addition, another limitation of UAV is endurance, a common battery-powered UAV can only support a flight for 15 to 30 minutes. Images acquired from different acquisition time may affect quality of data. Based on the reasons above, this research proposes a novel methodology to implement an algorithm for UAV flight planning in mountainous areas to filter out redundant data and design the path with shortest flight time under ensuring the quality of data. The Digital Surface Model (DSM) of the study area, user-defined GSD and overlap percentage will be used as the initial input of the algorithm. According to input parameters, the algorithm can calculate the position of all viewpoints in the flight mission. However, this initial dense viewpoint network does not show a significant improvement in accuracy or coverage. At the same time, intensive sampling based on this network will cause data redundancy and increase the time for both data acquisition and image processing. Therefore, one of the functions of the algorithm is to filter out those redundant images. For this purpose, principle for coverage check is proposed, that is all the points in study area need to be covered in at least "n" images. The filtering procedure works following this principle to remove those redundant images. Then, for all reserved viewpoints, using Simulated Annealing Algorithm (SAA) to design the optimal path with the shortest flight time. The final output of the algorithm is an optimal flight path composed of the position of all the points for acquiring images. The algorithm has been implemented in MATLAB. All the tests were performed on synthetic DSM with different shapes and terrain, in order to test the performance of the algorithm in different scenarios.

Keywords: UAV photogrammetry; Flight path planning; Algorithm implementation; Simulated Annealing Algorithm； Mountainous areas

.

ACKNOWLEDGEMENTS

Thanks to my parents and friends for their unfailing love and support. For so many years, they have always been supporting me and respecting me. Their love and care are the greatest fortune of my life.

Thanks to my supervisor, Dr. F.C. Nex for his numerous invaluable guidance and important suggestions throughout the journey. In the course of this research, his strong support and help contributed to the successful completion of the research. Thank you for his continuous encouragement and perseverance so that I can continue to move forward in the face of difficulties.

Thanks to my second supervisor Dr. V.V. Lehtola for the suggestions and help when I was confused. In the course of this research, he provided many good methods to stimulate my research ideas.

Thanks to my chair Prof.Dr.ir. M.G. Vosselman for the critical questions and helpful suggestions.

Thanks to drs. J.P.G. Wan Bakx for all the work he did for me.

Thanks to all the staff of ITC for making my entire journey here very pleasant and comfortable.

Thanks to all my friends in Enschede. They have provided me a great deal of help and encouragement during these two years. Because of their company, this journey has a lot of fun.

Finally, thanks to all the strangers who never knew each other for their brilliant smile and selfless help.

TABLE OF CONTENTS

LIST OF FIGURES

LIST OF TABLES

1. INTRODUCTION

1.1. Motivation

Unmanned Aerial Vehicle (UAV) is a type of aircraft without human pilot onboard. More accurately describe it should be Unmanned Aircraft System (UAS), which include a UAV, a ground-based controller, and a system of communications between the two (Gupta et al., 2019). The original aims to develop the UAV systems were for the military applications (Wallace et al., 2012). Nevertheless, the ability to remotely control an aerial vehicle is especially significant for other applications, like agriculture, transport, aerial photograph, etc. Due to the flexibility, high-efficiency and low-cost of UAVs (Stocker， C et al., 2019), their use rapidly extending to Geomatics area, such as forestry (Wallace et al., 2012), traffic monitoring (Heintz et al., 2007) and emergency management (Eudossiana & Planning, 2008).

As no human pilot onboard, the core content of UAV flight planning is algorithm(Qu et al., 2005a). Path planning is considered as optimization problems in the algorithm (Castillo et al., 2007). There are many kinds of algorithms used for solving it, which are mainly divided into the greedy method and the heuristic method (Caprara et al., 1999). The greedy algorithm starts with a certain solution, which can be given or be constructed in a certain way, and improve it by making a few modifications. For some problems, they are able to find the optimal solution, while for others, they stop at the local optimal solution (Zhang et al., 2000). In the optimization problem, when the optimal solution cannot be found, a heuristic algorithm can be used to find a solution close to the optimal solution. These algorithms are getting closer and closer to the optimal solution as they processing. In principle, if they run for an infinitely long time, they will find the optimal solution. Their advantage is that they can find a solution very close to the best solution in a short time (Lin & Kernighan, 1973).

Photogrammetric, as a common technique for data acquisition in Geomatics, can be operated by UAVs. Since Przybilla and Wester-Ebbinghaus firstly attempted UAVs for photogrammetric applications in 1979 (Eisenbeiss, 2004), it has been a popular measurement instrument. Particularly, in recent years, the combination of UAV platform and Global Navigation Satellite System (GNSS) system has greatly reduced the cost of UAV positioning, making it more widely used in photogrammetry. The characteristics of UAV photogrammetry can be summarized as follows:

1. **Rapid response capability.** UAV photogrammetry usually travels at low altitudes. There are no strict requirements for the launching and landing sites. The preparation time for flight is short, the operation is simple, and the transportation is convenient;
2. **Outstanding timeliness.** Traditional high-resolution satellite remote sensing data generally faces the problem of poor timeliness. UAV photogrammetry can be taken at any time and completed quickly in a short time;
3. **Limitations in study area.** The flight of aerial-based photogrammetry is usually several kilometers, which inevitably has the effect of clouds, while UAV often fly less than 100m, with much higher image quality and accuracy. Due to the limitation of flight height and its endurance, the stud area of UAV photogrammetry is quite small;

4. **Capabilities for fast data acquisition and modeling**. UAV platform is usually equipped with a digital camera, which can quickly acquire very-high resolution digital images and high-precision positioning data for generating DEM, orthophoto, and 3D models (Díaz-Varela et al., 2015).
With the combination of UAV photography and computer vision, the research on UAV has exponentially grown in recent years (Ham et al., 2016). The GNSS-equipped UAV can quickly and accurately capture images with very high resolution, providing high-quality data for 3D reconstruction. For different fields, no matter in forest monitoring (Dandois et al., 2015), indoor navigation (Wang et al., 2013), or research on landslide (Ruggles et al., 2016), the outputs of UAV-based on the images are always the accurate models. The quality of the final production generated from UAV images is not only related to image analysis technology, but also the flight planning at data acquisition.

The main task of photogrammetry is to calculate the three-dimensional object (terrain) co-ordinates for any object point represented in at least two photos (Linder, 2009). Therefore, one of the most important parameters of photogrammetry for data quality is the images overlap. Images overlap include frontal overlap (with respect to the flight direction) and side overlap (between flying tracks). To ensure the stereoscopic coverage, and to prevent gaps from occurring in the stereoscopic coverage due to tilt, flight height variations, and terrain variations, the minimum frontal overlap is 60% (much higher when images using for 3D model). Side overlap is required in photogrammetry to prevent gaps from occurring between flight strips, the suggest value is 20%-40% (higher when using for 3D model). The other is Ground Sample Distance (GSD), which is the distance between two consecutive pixel centers measured on the ground. The bigger the value of the image GSD, the lower the spatial resolution of the image and the less visible details. Consistent GSD makes a good quality final output, otherwise there will be lots of distortions on the output.

As the advantages of UAV platform mentioned above, UAV has become one of the most popular tools using for photogrammetry. The biggest difference between UAV-based photogrammetry and traditional aerial photogrammetry is the flight height. In traditional photogrammetry, the Area of Interest (AOI) is assumed to be a plane because the fluctuations of the ground are negligible compared to the flight height. This assumption is not valid when UAV images are considered: the flight height of UAV and the terrain undulations are very often of the same order of magnitude (i.e. 50-100 m), giving irregular image overlaps and different resolutions on the ground. As shown in Figure 1.1, in flat terrain (a), two consecutive photos have enough overlap, and GSD is same in both images; but in mountain area (b), due to the influence of terrain fluctuations, some overlapping between two images decrease, resulting in some points that cannot be observed in two images. In the case where all other parameters are the same, the higher the flight height means the larger GSD but smaller resolution. It can be found that GSD2 in (b) is smaller than GSD1 in (a), due to the different distance from drone to ground caused by terrain. All these problems affect the final quality of the photogrammetric outputs. Insufficient overlap leads to the lack of some points during data processing, which will affect image stitching and stereo mapping. Different GSD in images acquired from the same flight mission result in difficulties in automated tie-points matching, increasing the difficulty of feature extraction, finally affect the quality of output. What's worse, if the GSD is very different or overlapping missing too much, the automated tie-point extraction may fail, resulting in an unsuccessful generation of models.

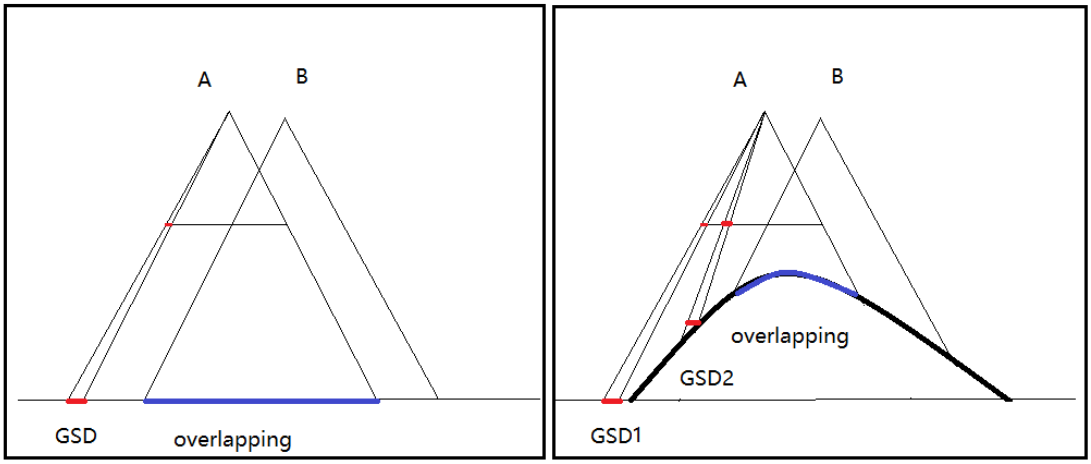

(a) (b)

Figure1. 1 The influence of terrain on UAV photogrammetry (a. flat area b. mountain area)

The flight plan is defined as "a time-ordered list of orders that a drone has to complete to fulfil the designed mission (i.e. take off, go to a waypoint, then hover to take a picture, then reach a second waypoint, then hover again to take a picture, finally land), while a trajectory is defined through the time-sampled dynamic state variation of the drone along time" (Besada et al., 2018), which include a number of viewpoints where the images will be captured. In field applications, in order to ensure the quality of the results, researchers often generate a denser viewpoints network, which means a higher image overlap. For example, in a research using UAV for geological mapping in Rodoretto Valley, Northwest Italian Alps, the authors set 80% image overlap in both frontal and side overlap (Piras et al., 2017a) , and another research using UAV photogrammetry for glacier monitoring in Switzerland, the overlap was taken as 80% (Baltsavias et al., 2001). These dense viewpoints will cause the redundant data, which increases the flight as well as the time of the subsequent image analyzing without improving accuracy or coverage (Alsadik, 2014). Furthermore, another challenge for UAV photogrammetry is energy. The battery-operated UAVs can typically support a flight between 15 to 30 minutes (Morbidi et al., 2016) and it is far from enough, obviously. Hence, it is necessary to find the minimum number of images to ensure the image overlap and the most efficient path during flight in mountainous areas.

In the field of geoinformatics, high-quality data can often provide products with high precision, high resolution and closer to the real situation. The generation of high-quality digital geographic products is not only related to the technology of data processing, but also depends on the method of data collection. This thesis attempts to study how to efficiently collect high-quality datasets using UAV as a platform in photogrammetry.

According to what mentioned above, this research attempts to develop an algorithm which could optimize UAV flight plan for acquiring images using for generating orthophoto, point cloud or 3D model in mountainous areas. The approximate Digital Surface Model (DSM) of an unknown mountainous area will be taken as the initial input for the algorithm. From the DSM, based on the GSD and image overlap required by user, the algorithm will compute the location of all viewpoints for the flight mission. Then, the algorithm will remove those redundant images to find the minimum number of images that can well-cover the input DSM. Finally, the algorithm will design an optimal flight path. The output of the algorithm will be an optimal flight path composed of the position of all the points for acquiring images.

1.2. Problem Statment

As UAV joint photogrammetry as a new platform, related technologies and concepts are also need to be updated. UAVs have the ability to perform efficient, flexible, and low-cost data acquisition, but they also face a number of challenges, such as poor endurance, limited measurement range, large impact by weather, and quality of results strongly affected by terrain, etc. As mentioned in section 1.1, the relief of terrain may cause problems with insufficient image overlap and different GSD in images, affecting the quality of final outputs. In order to eliminate the influence of terrain in the mountainous areas, ensuring the quality of data, the image overlap in real flight will often be much higher than suggested, which lead to a redundant data, increasing the time in both flight and data processing. And due to the limitation of battery life of UAV, it cannot fly for a long time. Thus, an efficient flight planning is needed to complete flight missions with the shortest flight time of UAV. In order to acquire high quality UAV images, this research attempts to develop an algorithm which could optimize UAV flight plan for acquiring images using for generating orthophoto, points cloud or 3D model in mountainous areas. The algorithm is able to compute location of viewpoints, filter redundant images and design optimal flight path.

1.3. Research Objective and Questions

1.3.1. Research objective

The main objective of this research is to implement an algorithm for UAV flight planning in mountainous areas to ensure the quality of final productions like orthophoto, point cloud or 3D model. The algorithm will take DSM of the Area of Interest (AOI) as input. Since the AOI is no longer a flat plane, in order to minimize the impact of the terrain, the gradient and elevation information in the area are calculated from the DSM, combined with the GSD requested by user, to calculate the relative flight height above the ground to eliminate the inconsistent GSD caused by the terrain fluctuation. Then the algorithm will compute the dense viewpoints network for image capturing, and have ability to filter out redundant images to minimize the number of images. After that, the algorithm will calculate an optimal flight path. The final output of the algorithm is an optimal flight path composed of the position of all the points for acquiring images.

1.3.2. Research questions

The main objective is divided into the following sub-objectives with corresponding research questions:

Sub-objective 1: The synthetic DSM need to be generated as AOI.
Corresponding questions:

- What are the advantages of using synthetic data?
- What type of DSM is suitable for this research?
- What is the best method for generating synthetic DSM?

Sub-objective 2: The algorithm should design a dense viewpoints network using for image acquisition which will assure the full coverage on the DSM.
Corresponding questions:

- What is the best overlap for the viewpoints network?
- How to evaluate the coverage of the network?
- How to reduce the influence of terrain on quality of results in mountainous?

Sub-objective 3: The algorithm should minimize the number of images by filtering out redundant data
Corresponding questions:

How to define the redundant data?
What is the best method to remove redundant data?
How to evaluate the completeness of the dataset after filter?

Sub-objective 4: The algorithm should design the optimal flight path to complete flight mission in the most efficient way.
Corresponding questions:

How to define the optimal flight path?
The shortest flight distance or the shortest flight time?
What is the best method to design the flight path?

Sub-objective 5: The performance of the algorithm needs to be tested in different scenarios to ensure the quality of the flight mission.
Corresponding questions:

How to evaluate the results of the algorithm?
How to build different test scenarios?

1.4. Novelty

Previous research on the use of UAV photogrammetry in mountainous areas to ensure the quality of output products by increasing the image overlap. Due to the undulating terrain of the mountains, the results of these researches will be more or less errors. At the same time, higher overlap refers to more images. Redundant images will increase flight time during data acquisition as well as the time for data analyzing. Additionally, limited by the endurance of the UAV, it is not possible to perform the flight mission for a very long time. From literatures what has already reviewed, most of the existing research focuses on the quality of data, the high resolution of the results, and the efficiency and accuracy of data processing, and there is a lack of research on the efficiency of image acquisition by drones. Thus, the proposed study aims to present a novel algorithm for UAV photogrammetry, which could automatically design flight plan in mountainous areas, optimize the minimum number of images and the most efficient flight path.

1.5. Data and Software

As this research does not focus on analyzing or extracting information based on existing data, but the general algorithm of data acquisition and all the work is done in a virtual environment through programming, so there is no requirement for data.
The code for the entire process was done in MATLAB R2019a. This was preferred since the study involved many matrix data to process. This also had the advantage of having numerous tools for image processing and in-built functions which became handy at times. Visualization of the data and results were easier to perform using these in-built functions and tools.

2. LITERATURE REVIEW

2.1. UAV photogrammetry

The developments of using UAV as a new aerial platform for data acquisition has been widely used in various fields because it can provide high-precision and high-resolution data sets (Colomina & Molina, 2014). Based on these centimeter-accurate digital models generated from UAV images, some research on subtle changes in the ground surface has been carried out. For example, a study in Morocco used high-accuracy DTMs generated from drone images and orthophotos to quantify soil erosion in the area (D'Oleire-Oltmanns et al., 2012); Peter et al. (2014) used UAV remote sensing data to evaluate the protective effect of land levelling measures on soil erosion; Stöcker et al.,(2015) combined the UAV images with additional terrestrial images and successfully generated the 3D model of the gully with a slope gradients of 50°-60° and 0.5 cm accuracy.

Another application for UAV photogrammetry is in mine areas. Esposito et al. (2017) use the Multiscale Model to Model Cloud Comparison (M3C2) tool from Software CloudCompare to compare the two point clouds data taken at different times. Calculating the excavated volume of mineral resources during two surveys based on the distance between two clouds. Hu et al. (2017). set up an evaluation system of using UAV for remote monitoring land reclamation in mining area, proposed that UAV technology is available for information investigation, geological hazard and pollution monitoring, land reclamation and ecological plan, reclamation acceptance and evaluation in mining area.

Based on the timeliness of UAV, Shunhai & Yao (2014) proposed a solution to the monitoring problem of land consolidation, using orthophotos produced by UAV photogrammetry to achieve short-term and comprehensive detection of construction areas.

There are many papers on terrain acquisition using UAV system. For angle constrained terrain mapping (Sujit et al., 2013), the authors implement a route planning algorithm that can determine efficient paths taking kinematic constraints of the vehicle and the angle of arrival. And for geological mapping (Piras et al., 2017b), a dense DSM (DDSM) and orthophoto were produced by the high resolution (4cm) photogrammetric acquisition images.

Some authors focus on UAV photogrammetry technology. Gülch (2012) built the Personal Aerial Mapping System (PAMS) consisting of a small fixed-wing UAV and a digital camera for DTM/DSM and orthophoto generation. Harwin & Lucieer (2012) proposed the combination of photogrammetry and computer vision, using detailed images captured from micro-UAV and multi-view stereopsis (MVS) technique to generate the dense point cloud which is able to monitoring sub-decimeter terrain change. Gruen et al. (2012) proposed a method for generating 3D models of historical buildings. First generate DTM based on the satellite image, and use the drone image to refine it into a high-resolution 3D model.

2.2. UAV flight plan

Path planning refers to a moving objective in a working environment with obstacles, given a starting point and an end point to find a most suitable path of movement, and moving the objective along the path can safely avoid the threat of obstacles. Path planning technology has a wide range of applications in many fields, such as automatic obstacle avoidance and penetration flight of UAVs; The missile avoids radar search, prevents being attacked, and completes the fixed-point blasting mission; Real-time road planning and navigation based on GNSS and Geographic Information System (GIS); Road network planning tasks during city construction; Distribution of transportation vehicles in logistics management systems and routing distribution in the field of communication technology. In a word, the planning problem about the topology of the point-line network can be solved based on the path planning method (Tsardoulias et al., 2016).

Since the poor endurance of UAV. There are many researches on UAV flight path optimization focuses on energy consumption. E-Spiral algorithm, implementing for accurate photogrammetry which considers the camera sensor and the flight height to ensure the overlapping of the flight mission, reducing energy consumption by using an energy model to set different optimal speeds for straight segments of the path (Cabreira et al., 2018). A survey on the minimum energy cost for irregular area for UAVs flight planning (Cabreira et al., 2019) proposed a Grid-based method solve the Cover Path Planning (CPP) problem in irregular-shaped areas, which the approach was able to save up to 17% of energy in real flight experiments.

Numerous studies focus on the optimization of flight path, like using Genetic Algorithms (Qu et al., 2005b) to get the optimal solution of flight path; Some research regraded flight planning as a classic optimization problem, the traveling salesman problem (TSP), and solved the problem by heuristic algorithms like Evolutionary Algorithms (EA) (Ólafsson, 2006), or Ant Colony Optimization (ACO) (C. Zhang et al., 2010). In (Li et al., 2011), authors transformed the problem from CPP for a convex polygon into width calculation of the convex polygon. Then developed an enhanced exact cellular decomposition method to find the flight path with the least number of turns. An accelerated A* (AA*) algorithm improved by removing the trade-off between the speed and the precision by introducing the adaptive sampling, significantly speeding up the calculation process (Sislak et al., 2009). In (Yang & Kapila, 2002), authors developed a 2D optimal path planning by simplified the problem from optimal path to parameter optimization, satisfying the UAV kinematic constraints and vector calculus. In other research (Ambrosino et al., 2009), an algorithm for generating 3D paths and tracking is proposed. The algorithm is able to satisfy any tracking form start point to end point at a given position and velocity. Keller et al. (2017) proposes an algorithm that combines image search technology with spline method, in order to solve the problem that the integrated sensors in the UAV system cannot meet the multipath planning in complex situations. The algorithm can continue to provide a feasible path for drones in more complex situations. Phung et al. (2017) proposes an enhanced discrete particle swarm optimization algorithm for improving the efficiency of solving the traveling salesman problem in UAV trajectory.

As a classic algorithm for solving TSP problems, Simulated Annealing Algorithm (SAA) is widely used for UAV flight planning. In (Turker et al., 2016), authors develop parallel SAA based on SAA, successfully solved the flight path planning for multiple UAVs. In a study of searching for the shortest UAV flight path while avoiding obstacles (Meng & Xin, 2010), The author incorporate Metropolis acceptance criteria of simulated annealing algorithm into genetic algorithm, compressed code space while getting a better flight path. Turker et al. (2015) using Simulated Annealing (SA) algorithm to obtain nearly optimal path

under regular circular radar threats in 2D environment. Behnck et al. (2015) used simulated annealing algorithm to solve the path planning problem of a group of small drones in cooperative flight, which is regarded as a multiple travel salesman problem

Several studies have focused on the problem of data redundancy caused by intensive sampling of UAV. In (Liu et al., 2019), authors proposed an optimal UAV data collection trajectory (OUDCT) scheme based on the matrix completion using to efficiently collect information in AOI. The OUDCT scheme can reduce extra data by 50%-52% while save the flight time by 17%.

Based on the literatures have been reviewed, UAV photogrammetry has been widely used in various fields. But research for UAV path planning mostly focuses on avoiding obstacles, improving the safety of flight path, and cooperative flight of multiple UAVs. Most research on UAV photogrammetry path planning focuses on the quality and resolution of the acquired data sets, and few studies focus on the data redundancy caused by intensive sampling of UAV photogrammetry.

3. METHODOLOGY

The key processes involved in this research are detailed in this chapter, as shown in Figure 3.1. The methods used for solving the specific problem will be introduced in following sections. In general, it starts from the generation of synthetic DSM as study area. Based on the created DSM, generating a dense viewpoints network for UAV photogrammetry. Then, some of viewpoints in network, whose captured image identified as redundant data will be removed from network. Finally, an optimal flight path for UAV to visit all retained viewpoints will be designed for image acquisition.

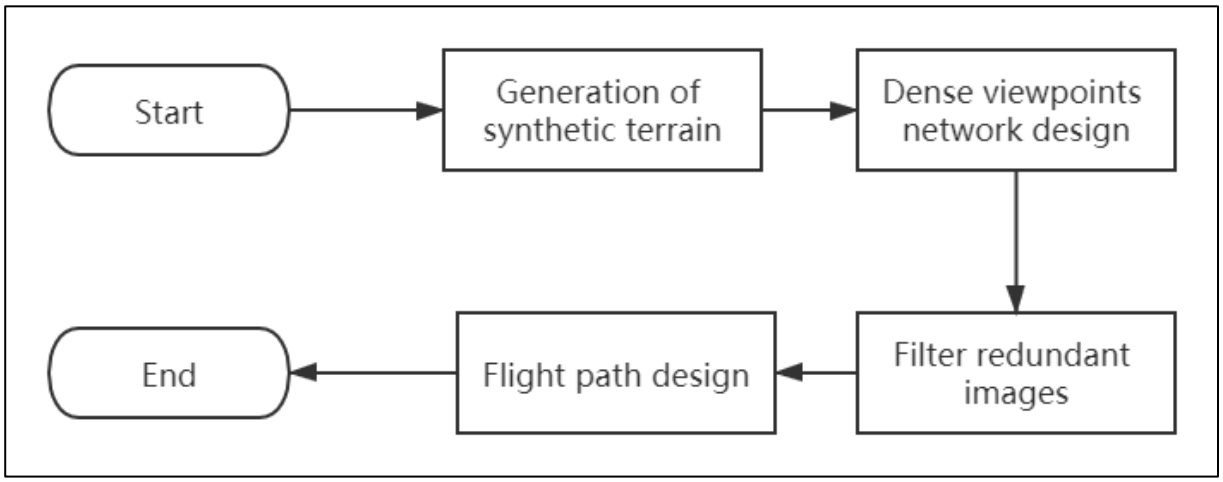

Figure3. 1 Genera overview of steps in methodology

3.1. Generation of synthetic terrain

Considering the generality of the algorithm required in this research, all the development and testing in Chapter 4 are based on the synthetic digital three-dimensional terrain model. The purpose of this section is to provide some methods for generating synthetic models, which mainly including continuous function models and interpolation. The advantage of these methods is that it can quickly and conveniently generate three-dimensional terrain models of different sizes and shapes, which greatly realizes the diversity and complexity of the terrain in the study area and enriches the test data samples. It is convenient to test the performance of the algorithm in different environments.

Interpolation refers to interpolating continuous functions on the basis of discrete data, so that this continuous curve passes through all given discrete data points. Interpolation is an important method for approximating discrete functions. It can be used to estimate the approximate value of the function at other points through the function at finite points. In this study, by defining the elevation values of some points in the study area, combined with the interpolation function in MATLAB, the interpolation work is completed and the undulating terrain model is generated.

The undulations of terrain can be described by mathematical models. For example, Equation (1) is exponential function, and Equation (2) is probability density function of binary Gaussian distribution.

$$z(x,y) = \sum_{i=1}^{n} h_i \exp\left[-\left(\frac{x-x_i}{x_{si}}\right)^2 - \left(\frac{y-y_i}{y_{si}}\right)^2\right] \quad (1)$$

Where, $z(x,y)$ refers to elevation value at this point in the study area;
(x_i, y_i) refers to the center coordinate of peak i;
h_i refers to terrain parameters;
x_{si}, y_{si} refers to attenuation of peak i along the x-axis and y-axis;
n refers to number of peaks

$$z = 3(1-x)^2 e^{-x^2-(y+1)^2} - 10\left(\frac{1}{5}x - x^3 - y^5\right)e^{-x^2-y^2} - \frac{1}{3}e^{-(x+1)^2-y^2} \quad (2)$$

Where, x, y refers to the coordinate of point
z refers to elevation value at this point

3.2. Dense viewpoint network design

In order to fully cover the AOI, a dense network of viewpoints will be designed firstly. The main process of design is shown in Figure 3.2. Some related parameters for designing viewpoints network are shown in Table 3.1. Since the camera model cannot be determined, the camera interior parameters cannot be defined. Instead, the input for the network design is the user's requirement of overlap percentage, flight height, the angle α between the viewpoint and the edge of the image in the vertical direction and approximate DSM of the AOI. Angle α is used to determine the range of the terrain model covered by the image taken at this viewpoint (Figure 3.3), including a total of two angles one for the frontal direction and the other for side direction, defined as α1 and α2 respectively. This angle could also be calculated by Equation (3) if the input data is GSD and focal length and image size. Flight height (H) should have been calculated in Equation (4) but directly given. In this research, the flight attitude of the UAV is a fixed flight height during flight mission. The relative flight height (H') equals the flight height (H) minus ground elevation (h). The number of images could be calculated by baseline length (L_b), gotten from Equation (5), while the number of strips could be calculated by the strip intervals (L_s), calculated by Equation (6). Because the camera parameters are not defined, Equation (5) and (6) need to be rewritten as (7) and (8), replacing the focal length and image size with angle α. Based on these information above, the final result is a network of all viewpoints with their coordinates.

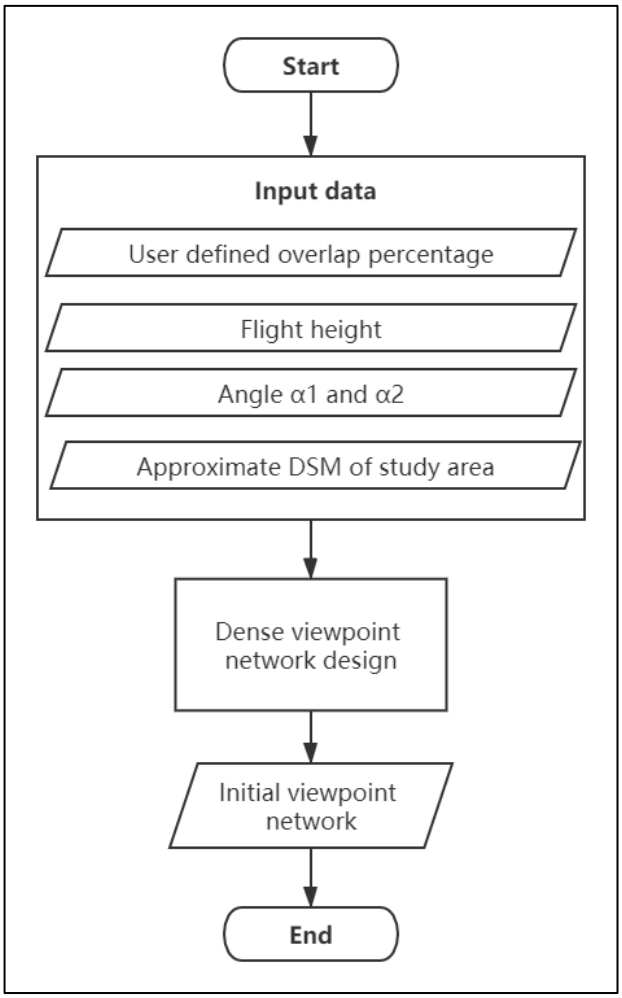

Figure3. 2 Flowchart for dense viewpoint design

Table3. 1 parameters for UAV photogrammetry

Type of parameter	Name	Symbol
Flight parameters	Flight height	H
	Flight speed	V
	Flight time	T
	Baseline length	L_b
	Strip intervals	L_s
Camera parameters	focal length	*f*
	Pixel size	a
	Camera rotation	Ω, Φ, K
	Image size	$C_A * C_D$
Performance parameters	Along track overlap	A
	Across track overlap	D
	Ground sample distance	GSD
Ground parameters	Ground elevation	h
	Gradient	G

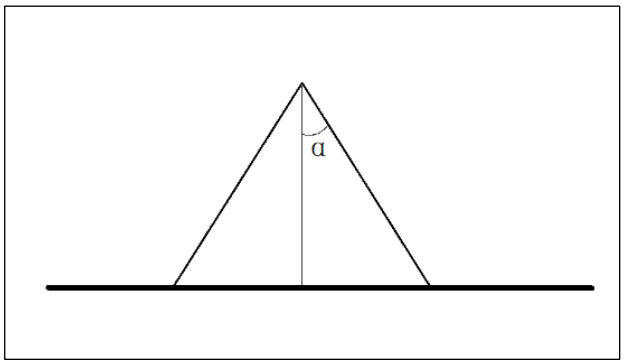

Figure3. 3 Diagram of angle α

$$\tan\alpha = \frac{1}{2}\mathrm{GSD}\cdot \mathrm{C/H} \tag{3}$$

Where, α refers to angle between the viewpoint and the edge of the image in the vertical direction;
GSD refers to ground sample distance;
C refers to image size;
H refers to flight height

$$\mathrm{H} = \frac{\mathrm{f} * \mathrm{GSD}}{\mathrm{a}} \tag{4}$$

Where, H refers to flight height
f refers to focal length
a refers to pixel size

Baseline length refers to the distance of lens between two consecutive shutters, can be calculated by the formula:

$$\mathrm{L_b} = \frac{(1-\mathrm{A}) * \mathrm{H} * \mathrm{C_A}}{\mathrm{f}} \tag{5}$$

Where, $\mathrm{L_b}$ refers to baseline length
A refers to along track overlap
H refers to flight height
$\mathrm{C_A}$ refers to image size along the strip
f refers to focal length

Strip intervals refers to the distance two adjacent strips, can be calculated by the formula:

$$\mathrm{L_s} = \frac{(1-\mathrm{D}) * \mathrm{H} * \mathrm{C_D}}{\mathrm{f}} \tag{6}$$

Where, $\mathrm{L_s}$ refers to strip intervals
D refers to across track overlap
H refers to flight height
$\mathrm{C_D}$ refers to image size across the strip
f refers to focal length

$$L_b = 2(1 - A) * H * \tan \alpha 1 \quad (7)$$

Where, L_b refers to baseline length
A refers to along track overlap
H refers to flight height
$\alpha 1$ refers to the angle between the line from the viewpoint to the edge of the image and the normal in the flight orientation.

$$L_s = 2(1 - D) * H * \tan \alpha 2 \quad (8)$$

Where, L_s refers to strip intervals
D refers to across track overlap
H refers to flight height
$\alpha 2$ refers to the angle between the line from the viewpoint to the edge of the image and the normal across the flight orientation.

The exterior orientation parameters for camera network were defined as follows. Omega (Ω) value for the quadcopter usually ranges from 0° to 90°. Ω value equals 0° refers to the camera is nadir to the ground while directly looking at horizon if it is 90°. This research only considered nadir view, so the value of Ω is always 0°. Phi (Φ) is defined based on the orientation of the facades to look in direction, it is also 0° for nadir view in the research. For the quadcopter that uses gimbal, Kappa (K) is 0°.

3.3. Filter redundant images

The principle of visibility check is to confirm whether all the points in study area were covered in at least n (natural numbers greater than 3) images. The dense viewpoint network generated in Section 3.2 does not show a significant improvement in accuracy or coverage, but also increases time in both data acquisition and image analyzing. Therefore, this study attempts to optimize the number of viewpoints, completing the flight mission with the minimum number of viewpoints while ensuring the quality of the data. We define that if an image in the dataset is deleted, the remaining images can still ensure that all points on the DSM of the can be observed by at least "n" images, then the deleted image is redundant data and can be removed, otherwise it will be preserved. By comparing the results of random deletion of an image, it is determined whether the image is redundant data. The specific process is shown in Figure 3.4 and explained below:

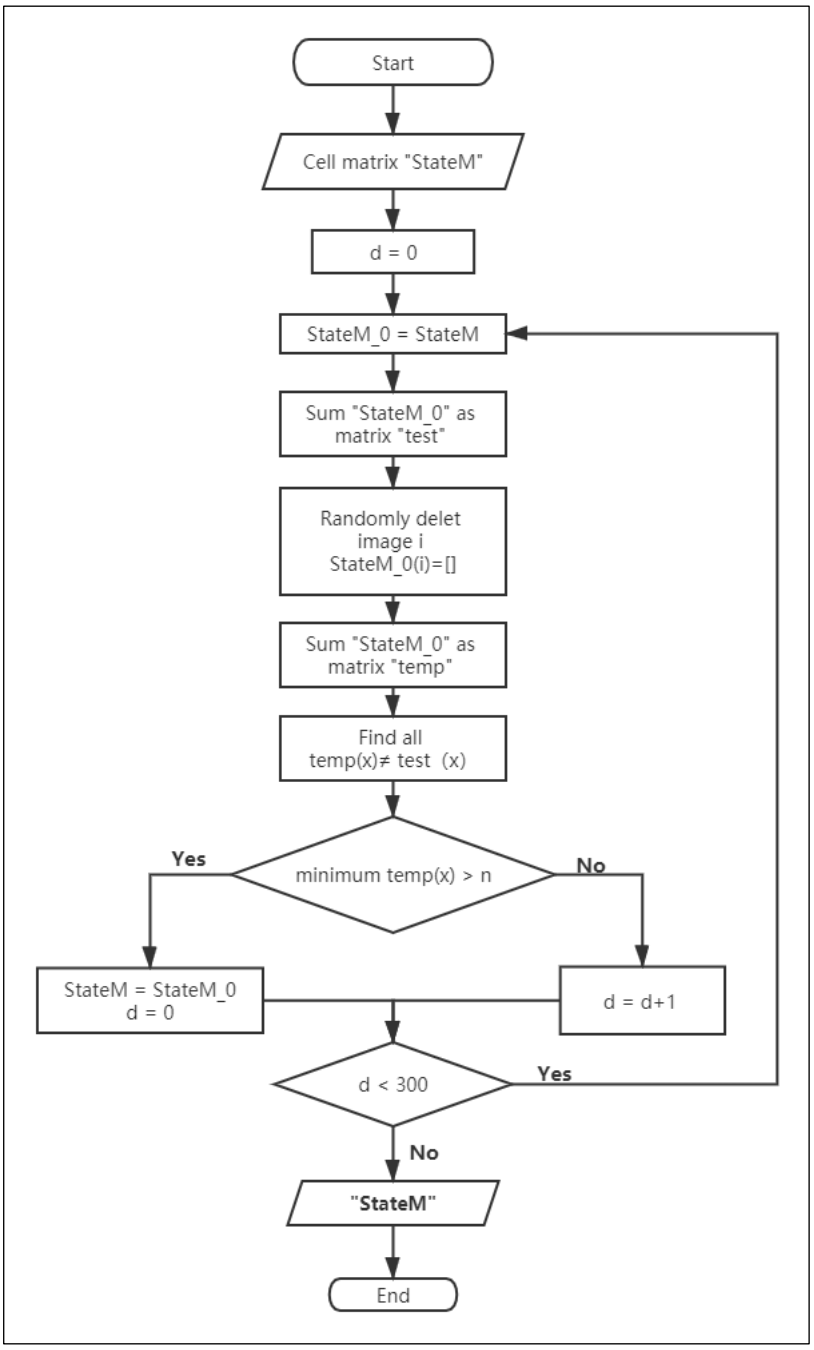

Figure3. 4 The workflow for removing redundant images

1. Definition of input data. The input data are approximate DSM of the AOI, flight height H, angleα1 and α2, and all the viewpoints with their coordinate. Assuming that the size of DSM is $l \times w$, the number of images is i. Creating a cell matrix (StateM) of size $l \times w \times i$ to represent the data set, each sub-matrix in it represents an image.
2. Coverage check. For each sub-matrix, the coverage area of the image on the synthetic DSM is determined by Equation (9) according to the given values of angle α1, α2 and flight height H. The value in the area covered by the image is 1, and 0 for outside the coverage area (Figure 3.5). In order to eliminate the influence of terrain on the coverage to the greatest extent, the relative flight height (the difference between the flight height and the ground elevation at this viewpoint) is used instead of the flight height for the calculation of the coverage area.

$$R = 2\tan\alpha \cdot (H - h) \tag{9}$$

Where, R refers to the range of coverage area for images;
α refers to angle between the viewpoint and the edge of the image in the vertical direction;
H refers to flight height;
h refers to elevation at this point

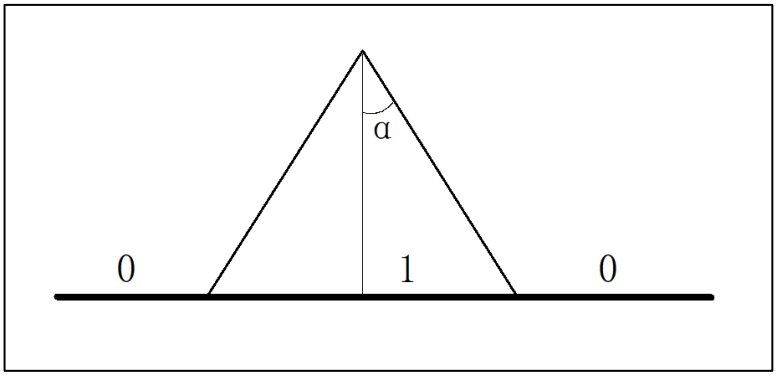

Figure3. 5 Diagram of image coverage

3. Sum all the sub-matrixes in the cell matrix "StateM" to get a new matrix (test), the size of the matrix "test" is equal to the DSM ($l \times w$), and each position in the matrix corresponds to the same position in DSM. The value of each position in the matrix represents the number of observation times for the corresponding position in the DSM. According to this matrix "test", the coverage of the entire study area was tested.
4. Redundant images filtering. A sub-matrix is randomly deleted from the cell matrix "StateM", and all the remaining sub-matrixes are summed to obtain a new matrix (temp). Retrieve the position of all unequal elements in the matrix "test" and "temp", that is, the range covered by the randomly deleted images. If all the values in the retrieved positions of matrix "temp" is greater than or equal to n (the minimum number of visible times), then the image corresponding to the deleted sub-matrix is a redundant image, delete both the sub-matrix and its corresponding viewpoint.
5. The loop will end after 300 consecutive times without deleting any image, and the result is viewpoints corresponding to the retained images after filtering.

3.4. Flight path design

As mentioned in the Chapter 1, due to the limitation of endurance, the UAV cannot fly for a long time. Therefore, this research purposes to design an optimal UAV flight path. Whether it is the shortest flight path or the shortest flight time, it is a reflection of the working efficiency of the UAV. However, compared to the flight distance, the flight time is closer to the state of the drone in actual flight, because when the drone turns, the flight distance will not increase but will consume time. Therefore, this study will use flight time as a constraint to design the optimal flight path of the UAV.

Based on the known coordinates of all the viewpoints after filtered, the flight plan can be described as a classic Traveling Salesman Problem (TSP) , that is, the UAV take off from the starting point, flies over each viewpoint only once and then returns to the starting point, how to design the flight path to minimize the total flight time of the UAV (Agatz et al., 2018). The TSP problem is a complete NP problem for the algorithm, that is, the worst-case time complexity increases exponentially with the increase of the problem size (Kirkpatrick & Selman, 1994). Currently, there is no effective traditional algorithm. Optimal solution calculation of the flight path requires the use of intelligent algorithms.

Simulated Annealing Algorithm (SAA) is an adaptation of the Monte-Carlo method (Metropolis et al., 1953), using for approximating the global optimum of a given function. It is a metaheuristic and often used in searching global optimization in a large discrete space. Due to the inherent limitations of traditional methods, many difficulties are encountered in dealing with TSP problems. Simulated annealing algorithm is an adaptive heuristic probabilistic search algorithm with multiple iterations. This algorithm provides a more scientific framework and an effective way to deal with TSP problems. When the simulated annealing algorithm is used to solve different forms of nonlinear problems, the global optimal solution can be obtained with greater probability.

The characteristic of the simulated annealing algorithm is that when looking for the optimal solution, it will not only accept a better solution, but also a probability to accept a worse solution (Dueck & Scheuer, 1990). This is used to jump out of the local optimal solution to find the global optimal solution (Figure3.6). The simulated annealing algorithm is inspired by materials science (Dai et al., 2013). Metal atoms at high temperature contain a lot of energy and have the ability to move and recombine randomly. As the temperature gradually decreases (annealing), this ability also decreases. When solving TSP, this feature will be considered as the possibility of accepting a worse solution. Therefore, the control parameters are the initial temperature, the end temperature, the cooling rate and the length of chain. The algorithm starts from the initial temperature, cools to the end temperature at the cooling rate, calculates the solution at each temperature with the iteration times equals length of chain, and finds the global optimal solution (McKendall et al., 2006), which is the flight path with the shortest flight time of the drone in this study. The input parameter of the algorithm at this stage is the viewpoint network after the redundant data filtering, and the output result is the flight path of the drone with the shortest flight time.

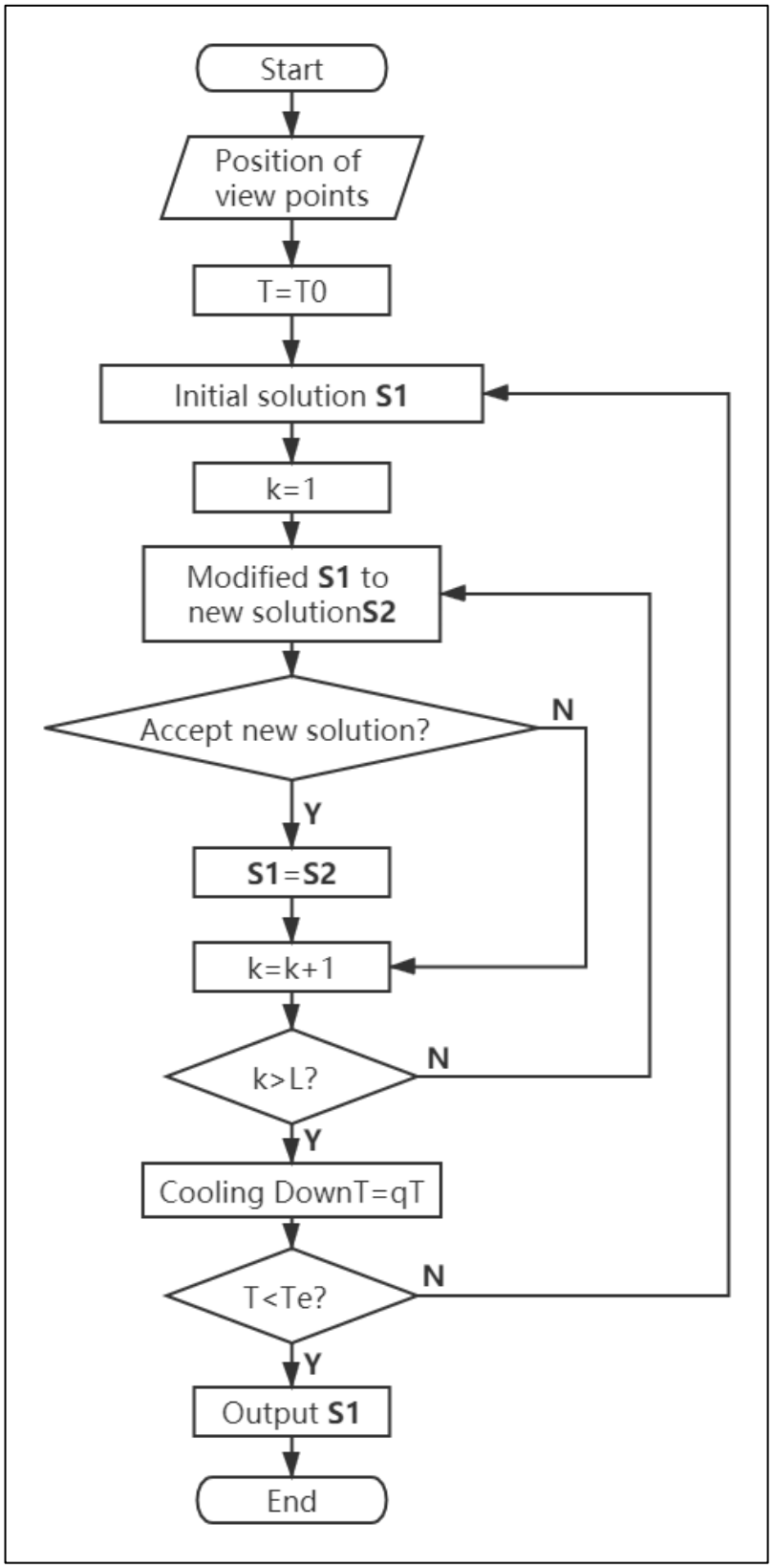

Figure3. 6 workflow for SAA

In order to reduce the calculation of the algorithm, the flight distance from each viewpoint to all the others will be calculated in advance. Figure 3.7 is the flow chart of the distance matrix calculation. The

input is the position of all viewpoints, and the output is a matrix of distances from each viewpoint to all the others.

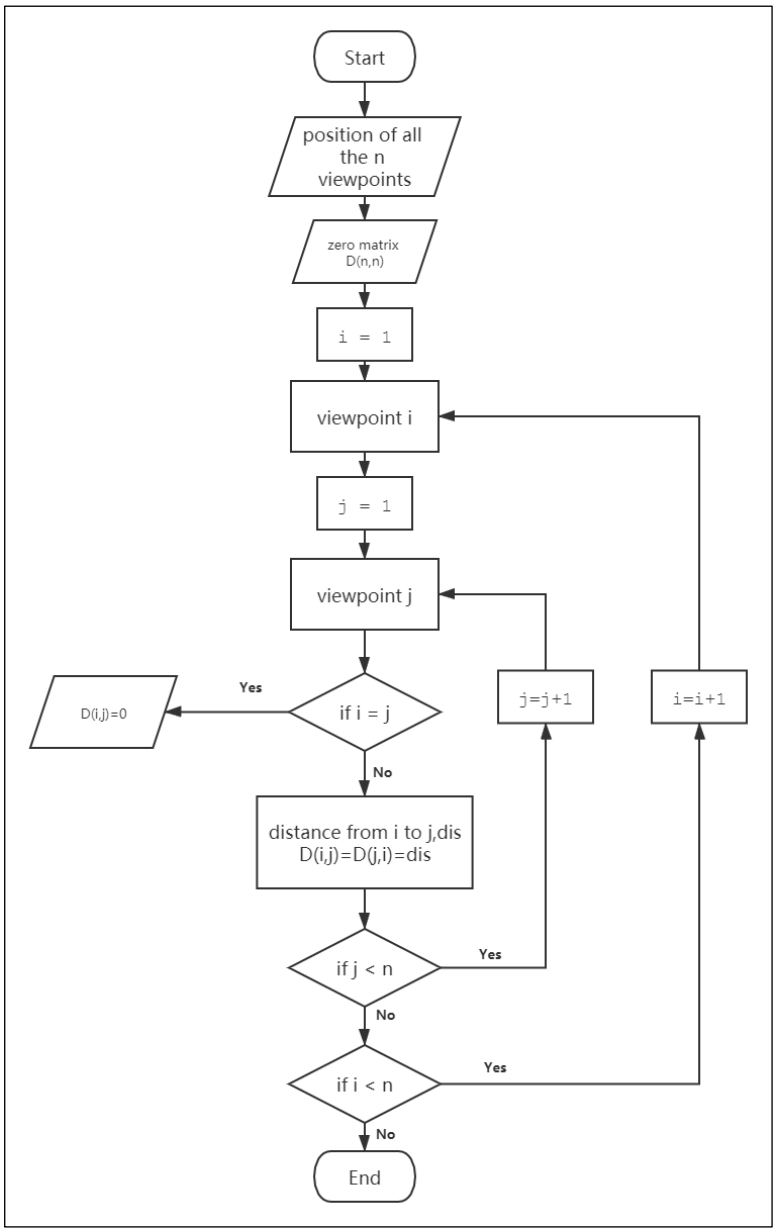

Figure3. 7 Workflow for Distance matrix

The realization process of the simulated annealing method in this study is as follows:

(1) Initialization: Define a sufficiently large initial temperatureT_0 and a sufficiently small end temperature T_e, let the current temperature $T = T_0$, the flight time under the conventional path as the initial solution S_1, determine the length of chain L of the Metropolis criterion, that is, the number of iterations at each current temperature.

(2) At the current temperature T, within the range of k = 1, 2, ..., L, repeat steps 3~6.

(3) Based on the current solution S_1, a new solution S_2 is obtained by choosing two points that are close to each other but not continuous in the flight sequence, insert the back point behind the other one.

(4) Calculate the increment of S_2, $df = f(S_2) - f(S_1)$, where $f(S)$ is the cost function.

(5) If $df < 0$, accept S_2 as the new current solution, $S_1 = S_2$; otherwise, randomly generate a number 'rand' uniformly distributed on (0, 1) and compare it with the acceptance probability $\exp(-df/T)$ at the current temperature T (Equation 10), if $\exp(-df/T) > \text{rand}$, accept S_2 as the new current solution, $S_1 = S_2$; otherwise keep the current solution S_1.

(6) Store the result S_1 at current temperature and cooling down. Reset S_1 equals conventional path. And back to step (2).

(7) End the loop when $T = T_e$, take the minimal value of all the stored S_1 as the optimal solution, end the program.

$$P = \begin{cases} 1, & \Delta E < 0 \\ exp\left(-\frac{\Delta E}{T}\right), & \Delta E \geq 0 \end{cases} \quad (10)$$

This research modified the algorithm to make it more suitable for the flight path planning of UAV photogrammetry:

1. Solutions are no longer randomly generated. For initial solution S_1, we use the conventional strip by strip path in photogrammetry, the flight trajectory looks like the letter "S". When generating new solution S_2, choose two points that are close to each other but not continuous in the flight sequence, insert the back point behind the other one.
2. The solution at the current temperature is no longer the initial solution for the next iteration. After each iteration, record the solution at the current temperature, and then reset the initial solution to the conventional strip by strip path at the start of the algorithm using for the next iteration. The output of algorithm will be a set of S_1 under different temperatures because of this improvement, and taking the minimum one as the optimal solution.
3. Increase the amount of calculations at each temperature, which is, the length of chain. Since the initial solution always be reset after each iteration, the calculation times in iterations need to be increased to ensure the accuracy of the results.
4. The end point is no longer fixed, the algorithm allows any point in the path to be the end point.

All these settings are because the traditional strip by strip flight path has already been an effective solution. In order to reduce the calculation amount of the algorithm, the optimization of the flight path is based on the traditional path to find a better result.

4. RESULTS

In this chapter, we created five scenarios with different DSM, percentage of overlap, etc. The results of each step under different situations involved in the research are detailed. All the key processes introduced in Chapter 3 were carried out step by step for different scenarios.

4.1. Generation of synthetic terrain

Figure 4.1 shows the synthetic DSM, which is using for test performance of the algorithm under five different scenarios. The size of Scenario Ⅰ, Ⅱ, and Ⅲ are 600×600m, as shown in Figure 4.1 (a), (b) and (c). Scenario Ⅰ is a flat ground to represent the standard environment. The peaks of Scenario Ⅱ are described by Equation (2), which can be directly realized by "peak" function in MATLAB. And the generation of Scenario Ⅲ is based on the Cubic Spline Interpolation method, which calculating elevation value in the study area from the value set at some points. These three scenarios are used to test the results of the algorithm under different terrain models. Scenario Ⅳ and Ⅴ have the same DSM, the size is 800m×400m (Figure 4.1 d). With the help of the mathematical model (Equation 1), by setting the parameters (Table 4.1) to determine the number of mountains and its height, center position and slope. The result shows the construction of mountains with different numbers, different elevations and slopes in a virtual environment. The above two scenarios are used to test the result if the minimum observed times for points on the DSM ("n" value in Chapter 3) is changed.

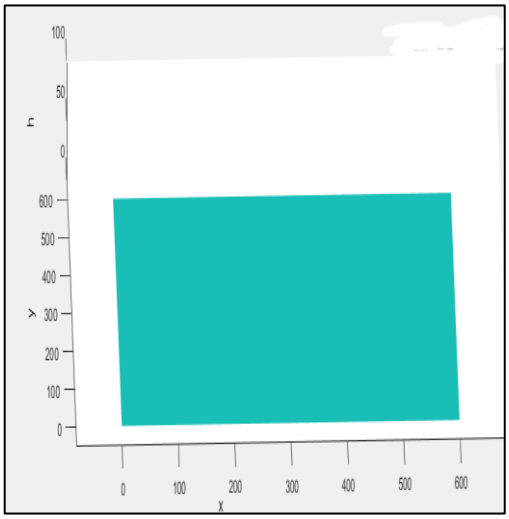

(a)

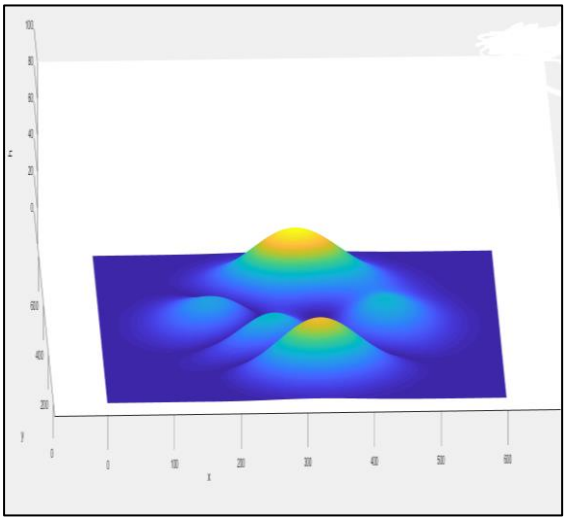

(b)

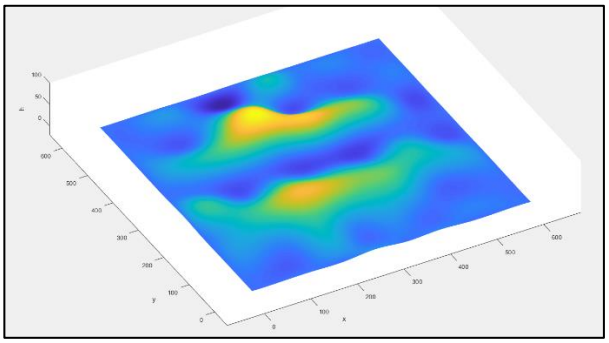

(c)

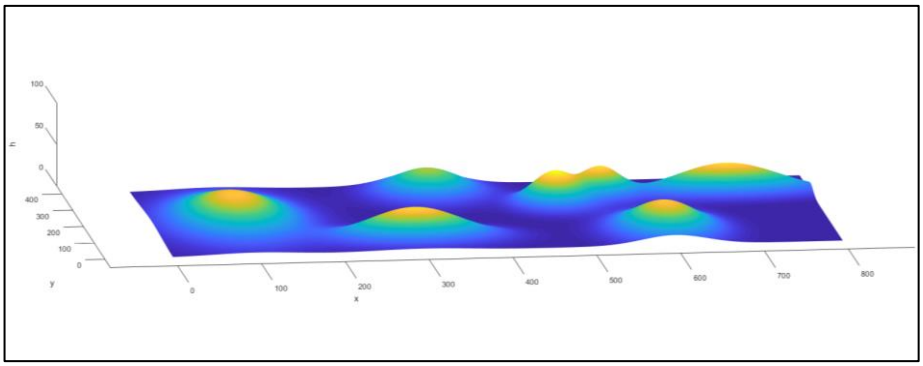

(d)

Figure4. 1 Synthetic DSM (a. Scenario Ⅰ b. Scenario Ⅱ c. Scenario Ⅲ d. Scenario Ⅳ and Ⅴ)

Table4. 1 Terrain parameters for Scenario

Parameters	Value
n	7
h_i	35; 35; 40; 33; 37; 29; 37
(x_i, y_i)	(200,100); (90,600); (260,490); (300,550); (300,700); (350,350); (80,300)
x_{si}	130; 85; 50; 42 ;37; 70; 50
y_{si}	70; 55; 39; 34; 90; 56; 80

4.2. Dense viewpoint network design

The input parameters for network design is overlap percentage, flight height, angle α1 and α2, and approximate DSM of the AOI. The settings of input parameters are listed in Table 4. Based on the given input parameters, the baseline length and the strip interval are calculated according to Equation (7) and (8). respectively, and combined with the coordinates of the initial viewpoint, a densely distributed viewpoint network within the study area is obtained (Figure 4.2). The number of viewpoints for different scenarios are shown in Table 4.2. As using same input parameters, the dense viewpoint networks for Scenario Ⅰ, Ⅱ and Ⅲ are the same, as well as Scenario Ⅳ and Ⅴ.

Table4. 2 Input parameters and results for dense viewpoints network generation

Parameters and results	Scenario Ⅰ, Ⅱ and Ⅲ	Scenario Ⅳ and Ⅴ
Overlap (frontal/side)	90%/70%	80%/50%
Flight height H	70m	70m
α1	38.5665°	45°
α2	38.5665°	30°
Number of viewpoints	779	319

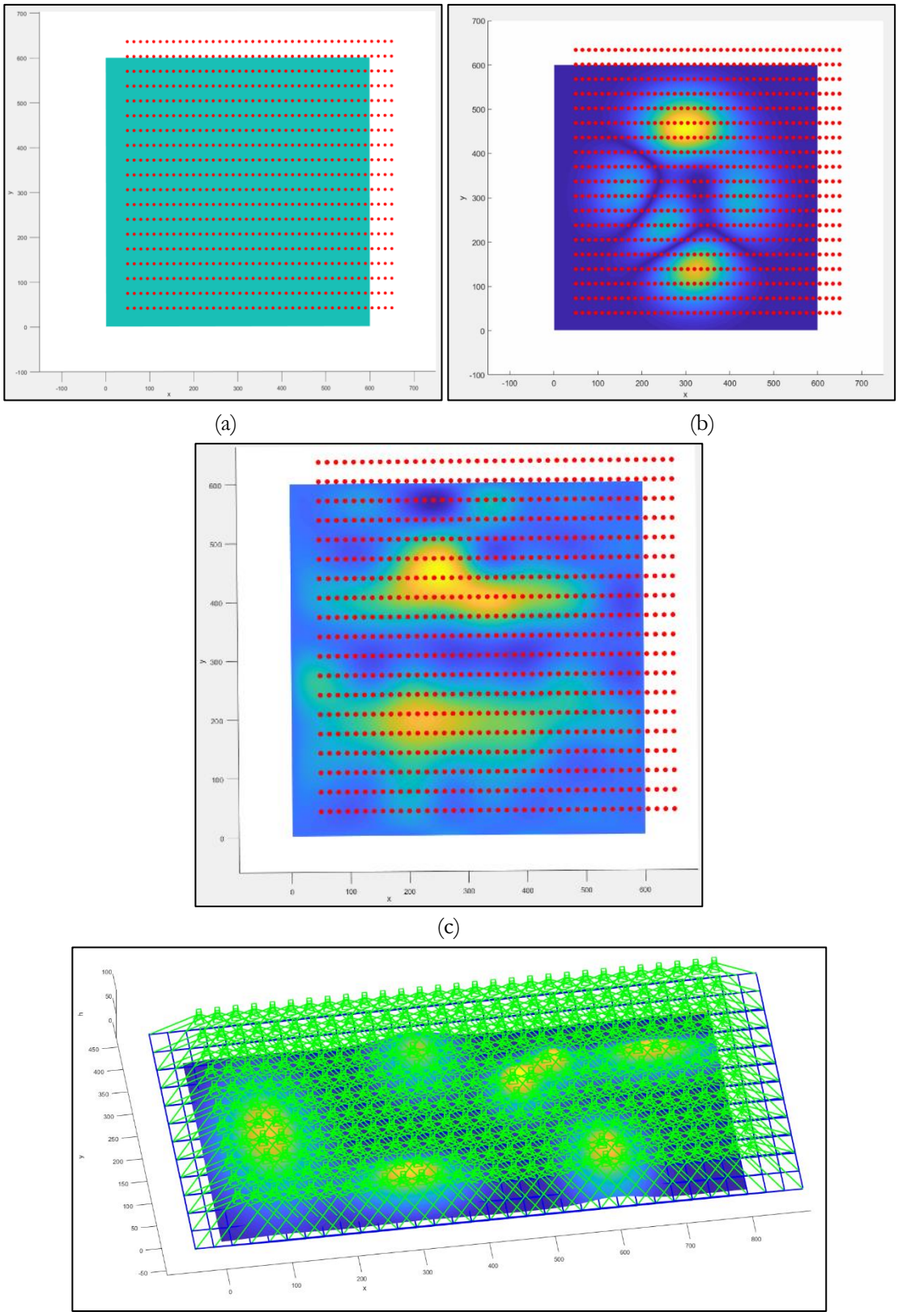

Figure4. 2 Dense viewpoint network distribution (a. Scenario Ⅰ b. Scenario Ⅱ c. Scenario Ⅲ d. Scenario Ⅳ and Ⅴ)

Coverage check for the first four scenarios, we defined that all the points in the created synthetic terrain are covered by at least 3 images to ensure that the group of images can be successfully used in the creation of the final digital products. That is, if an image in the dataset is deleted, the remaining images can still ensure that all points on the DSM can be observed by at least three images, then the deleted image is redundant data and can be removed, otherwise it will be preserved. Based on the definition above and coverage check method mentioned in Section 3.2, the results of coverage check before filtering are shown in Figure 4.3. In addition to the inevitable lack of coverage at the edge, all points in the study area for the first four scenarios were observed by at least 3 times, meeting the requirements of full coverage. But due to the coverage range of images is much smaller in mountainous areas, it will have less visible times in these areas, like Figure 4.3 (c) and (d). And for Scenario V, the minimum visible times is defined as 4, there will be some areas that are not completely covered (Figure 4. d). It means that the overlap percentage is insufficient.

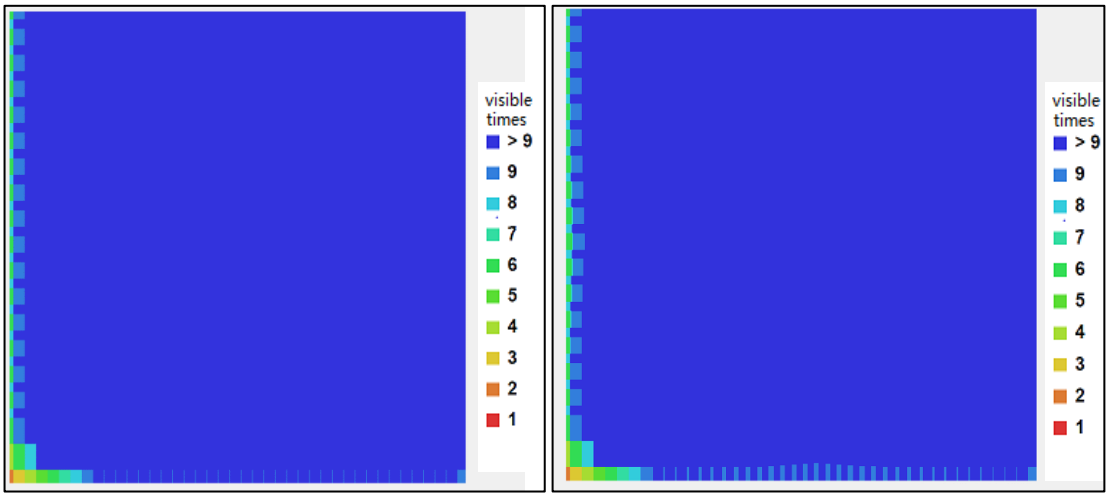

(a) (b)

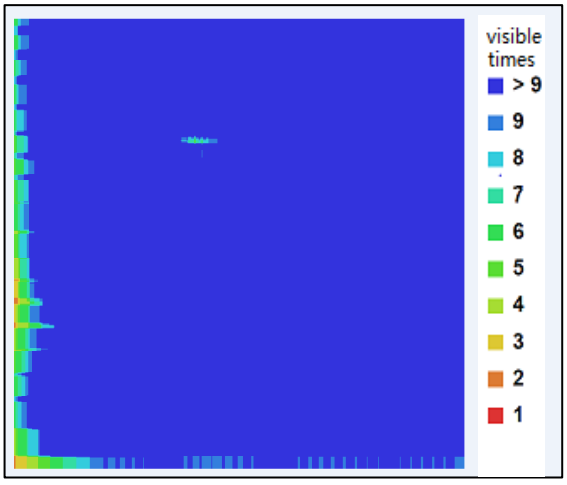

(c)

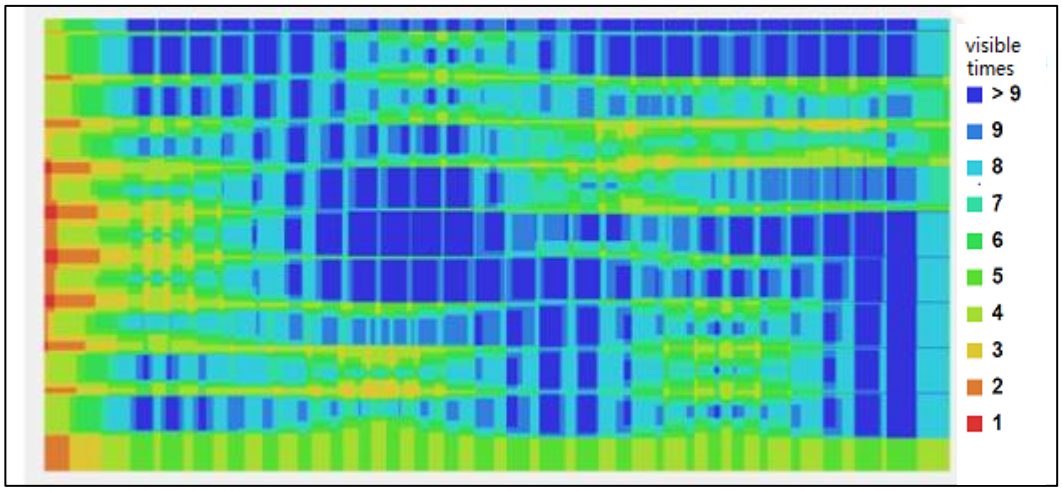

(d)

Figure4. 3 Coverage check before filter (a. Scenario Ⅰ b. Scenario Ⅱ c. Scenario Ⅲ d. Scenario Ⅳ and Ⅴ)

4.3. Filter redundant images

The processes of redundant images filtering followed the methods mentioned in Section 3.3. Decline in the number of viewpoints and data size for different scenarios are listed in Table 4.3 And the distributions of retained viewpoints are shown in Figure4.4.

Table4. 3 Comparison of filter result

	overlap/%	Data size		
		before	after	decrease/%
Scenario Ⅰ	90/70	779	155	80.1
Scenario Ⅱ	90/70	779	166	78.69
Scenario Ⅲ	90/70	779	185	76.25
Scenario Ⅳ	80/50	319	224	23.51
Scenario Ⅴ	80/50	319	305	4.39

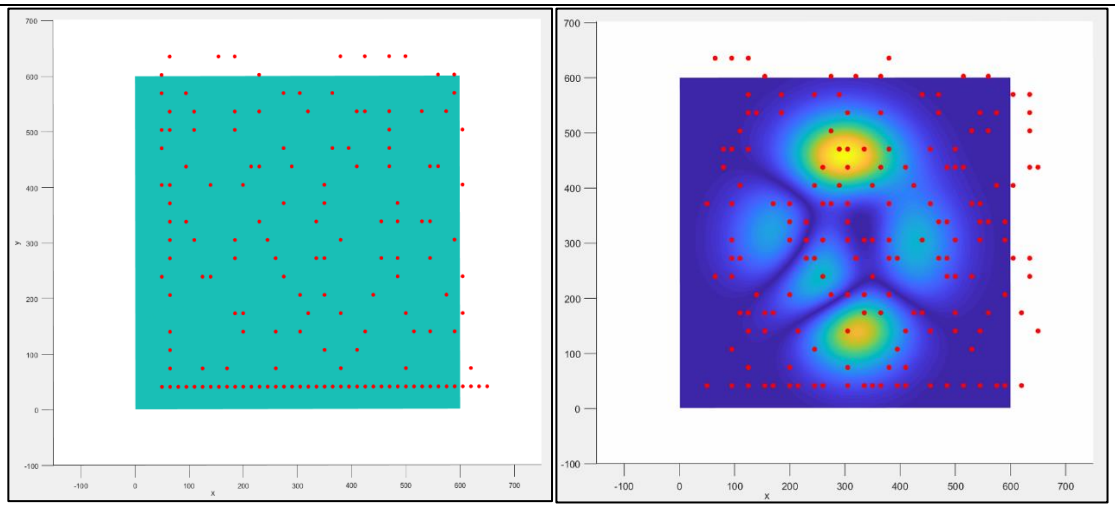

(a) (b)

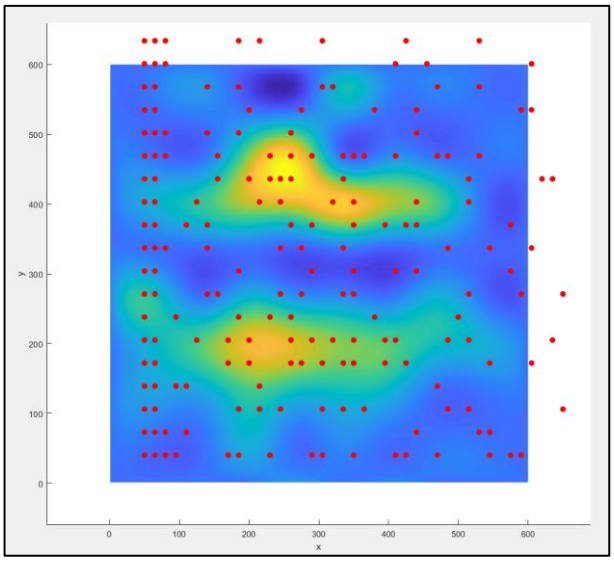

(c)

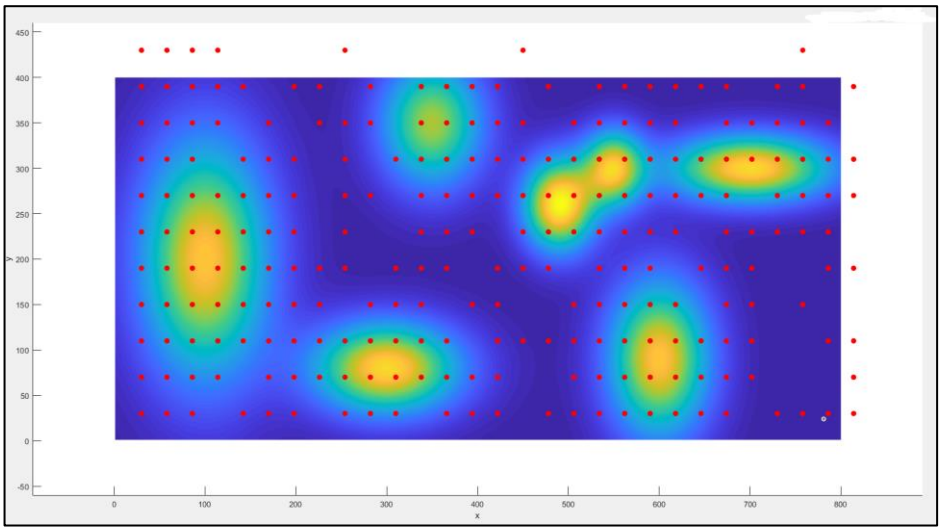

(d)

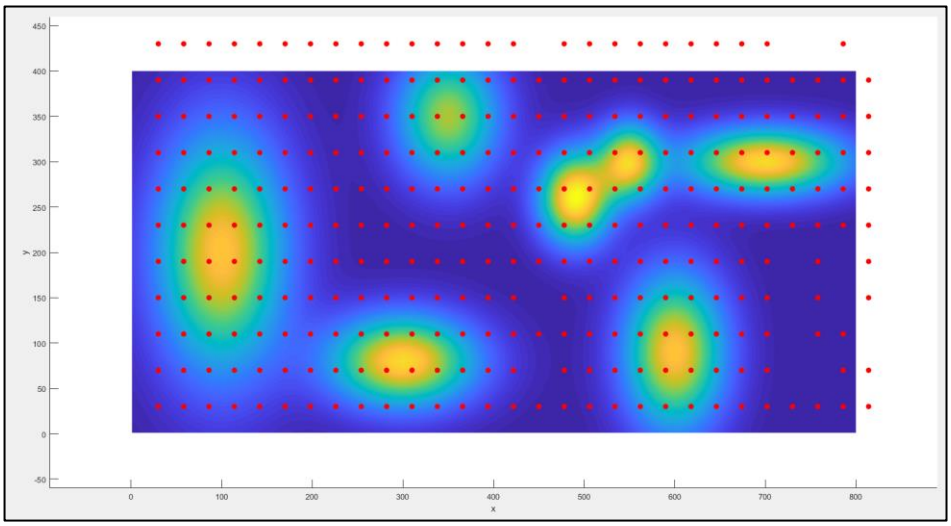

(e)

Figure4. 4 Results for redundant data filtering (a. Scenario Ⅰ b. Scenario Ⅱ c. Scenario Ⅲ d. Scenario Ⅳ e. Scenario Ⅴ)

Coverage check was performed on all the retained images again (Figure 4.5). In addition to the inevitable lack of coverage at the edge, all points in the study area for the first four scenarios were observed by at least 3 times, which still met the full coverage requirements. As for Scenario Ⅴ, except for those areas that were not completely covered in Section 4.2, no new areas were added.

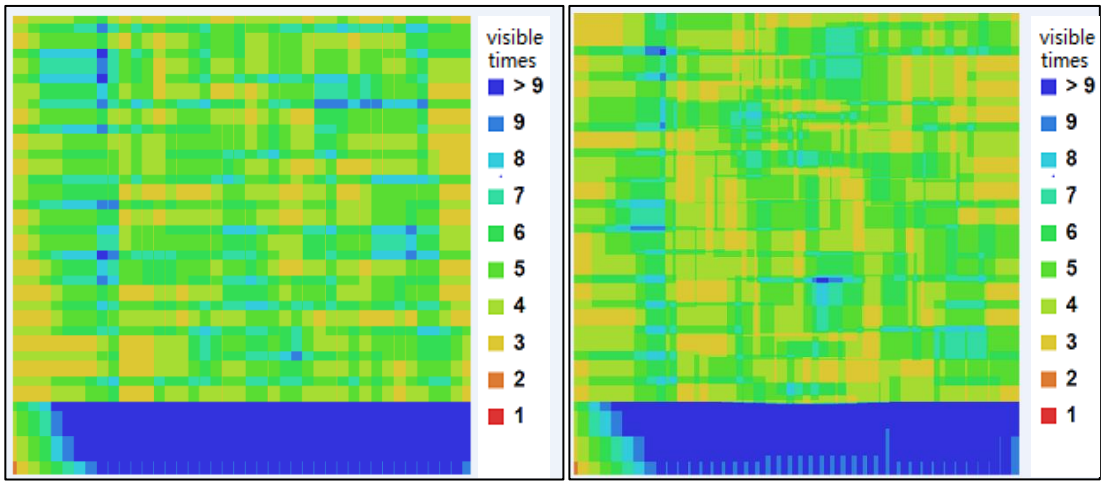

(a) (b)

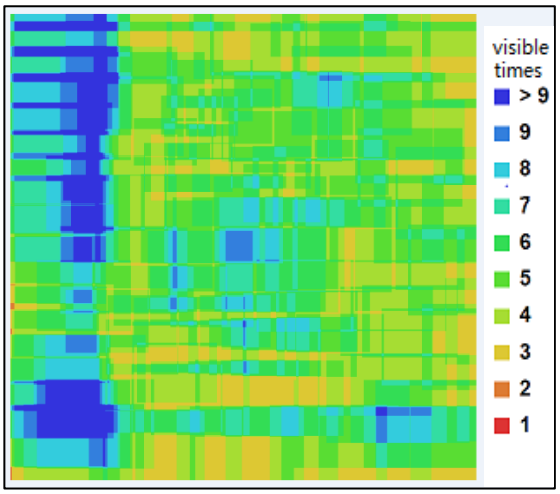

(c)

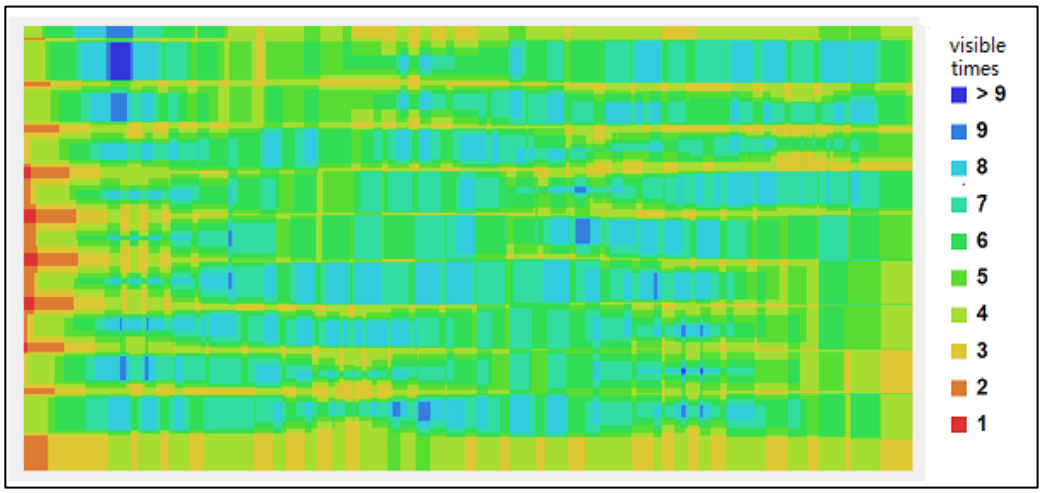

(d)

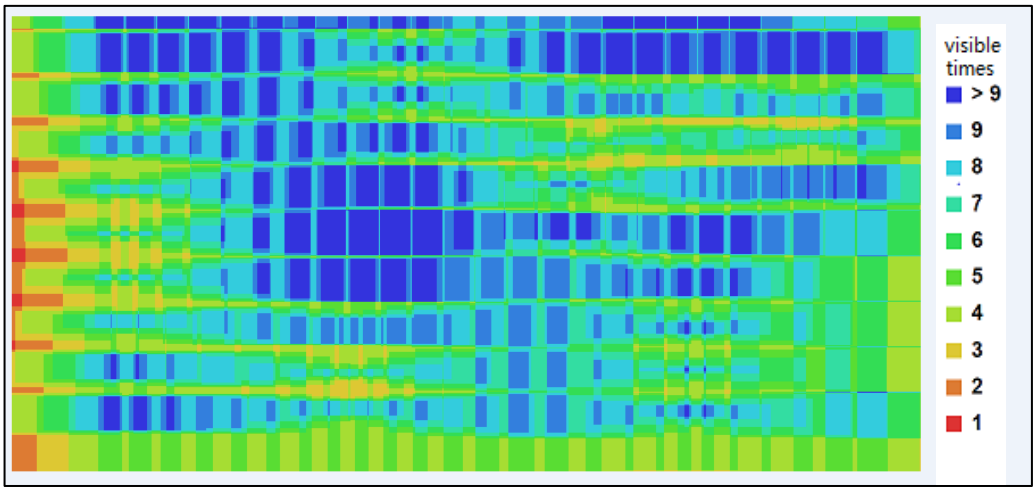

(e)

Figure4. 5 Coverage check after filter (a. Scenario Ⅰ b. Scenario Ⅱ c. Scenario Ⅲ d. Scenario Ⅳ e. Scenario Ⅴ)

4.4. Flight path design

In the process of UAV photogrammetry, the traditional strip by strip is generally adopted. Here we take Scenario Ⅳ as example (Figure 4.6), The UAV performs flight mission in the order from the smallest to the largest in the figure, starting from point 1 and passing through all target points to reach the end point 244. The time to perform the mission under this path will be used for comparison and analysis with the result of the shortest flight time path obtained in this research. In order to reduce the amount of calculation of the algorithm and avoid some unnecessary calculations, the path planning in this research is based on the optimization of the conventional strip by strip path to find a new path with a shorter flight time.

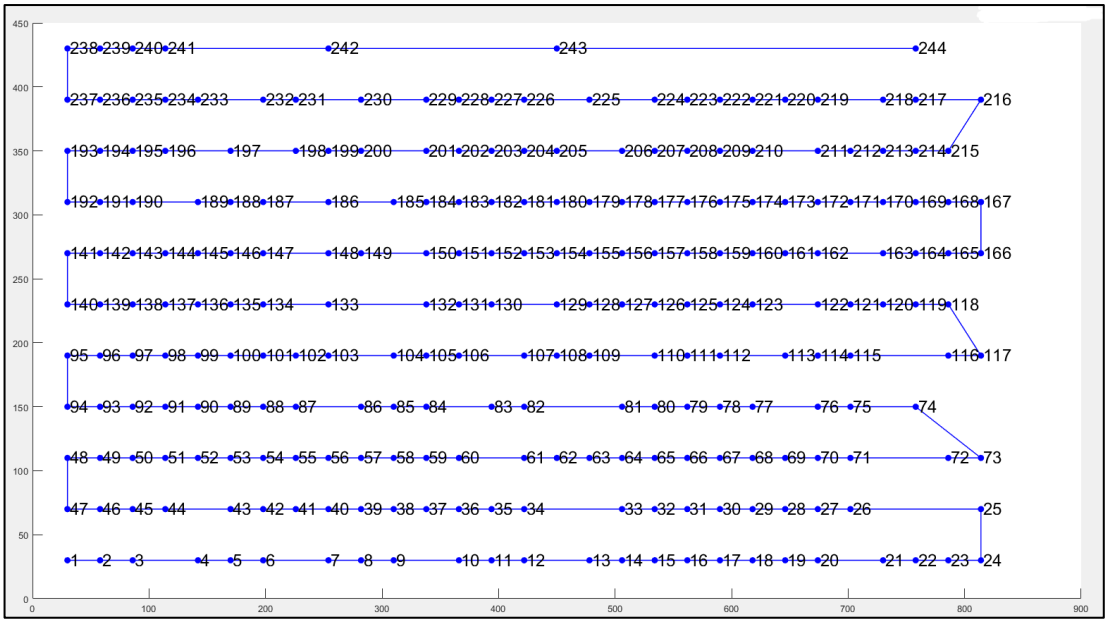

Figure4. 6 Traditional flight path as initial solution for SAA

In this study, the control parameter settings of the simulated annealing algorithm are shown in Table 4.4.

Table4. 4 Control parameter setting

parameters	value
Initial temperature T_0	2000
End temperature T_e	10^{-4}
Length of chain L	60000
Cooling down rate q	0.95

During the operation of the algorithm, it is assumed that the running attitude of the UAV is a uniform linear motion under ideal conditions, the flight speed is 5m / s, and the turning time is set to 5s. The flight time is the sum of the time required to depart from the starting point and traverse all the viewpoints to reach the end point. For any current point in the flight process, according to whether a triangle is formed between this point and its previous point and the next point to determine whether there is turning at this point.

The input of the algorithm is the coordinate information of all viewpoints after filtering and user-defined control parameters. The final output is the optimal path with the shortest flight time. The calculation results of flight time and time savings are listed in Table 4.5 The optimal path results are shown in Figure 4.7.

Table4. 5 Comparison of flight path design

	overlap/%	Flight time		
		Default path/s	Optimal path/s	Time save/%
Scenario Ⅰ	90/70	2288.2	2127.2	7.04
Scenario Ⅱ	90/70	2190.8	2080.3	5.04
Scenario Ⅲ	90/70	2399.97	2378.41	0.91
Scenario Ⅳ	80/50	1864.8	1756.33	5.82
Scenario Ⅴ	80/50	1895.37	1895.37	0

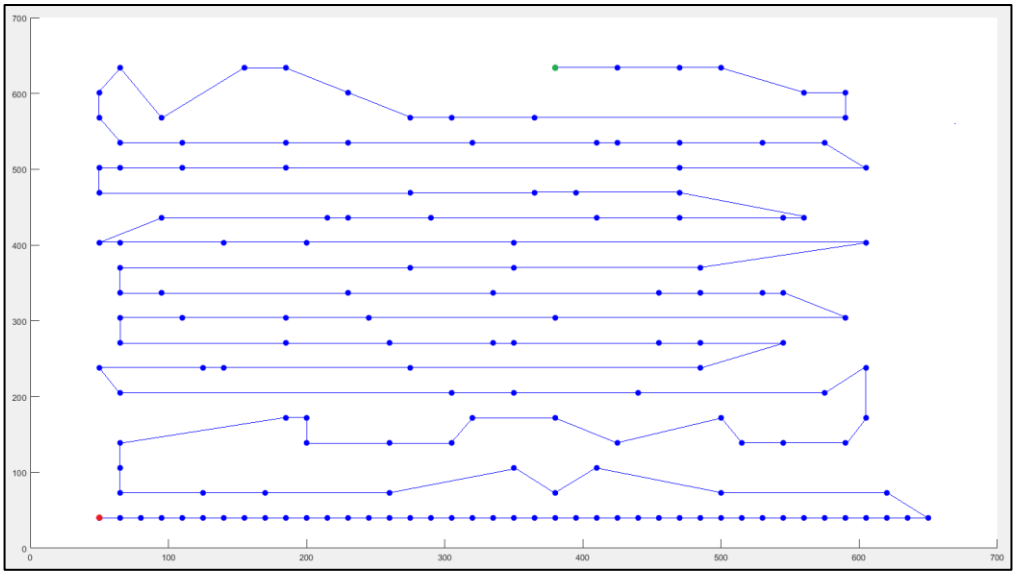

(a)

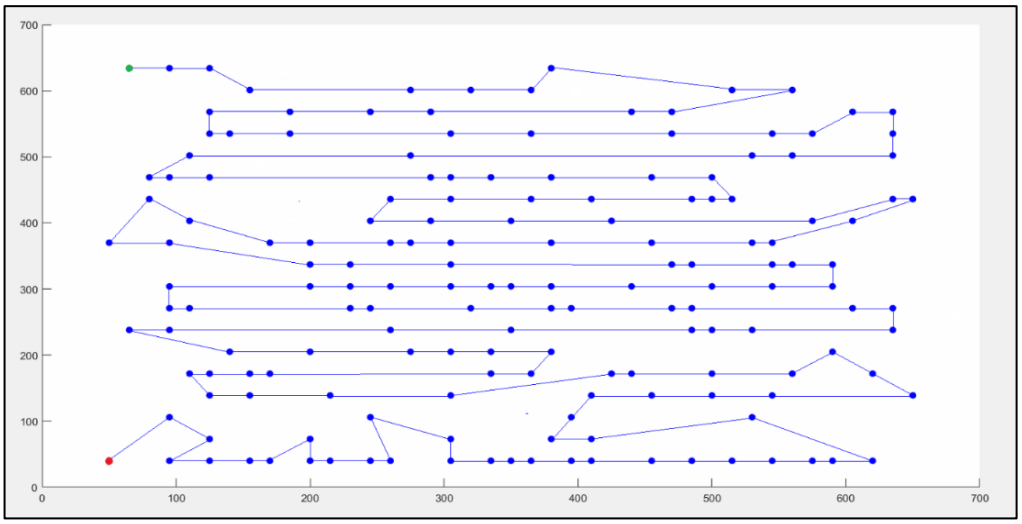

(b)

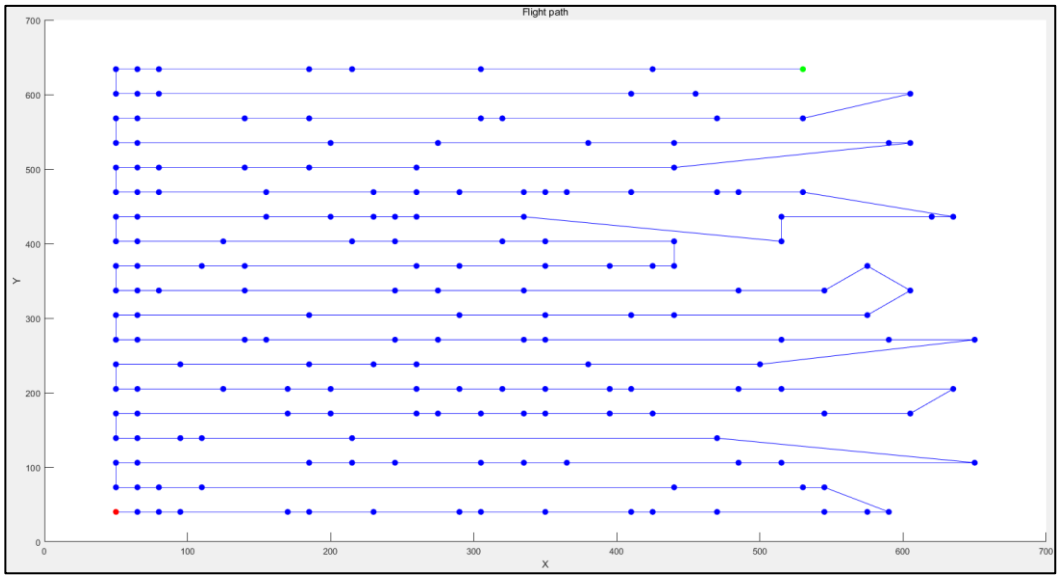
Flight path
X
Y

(c)

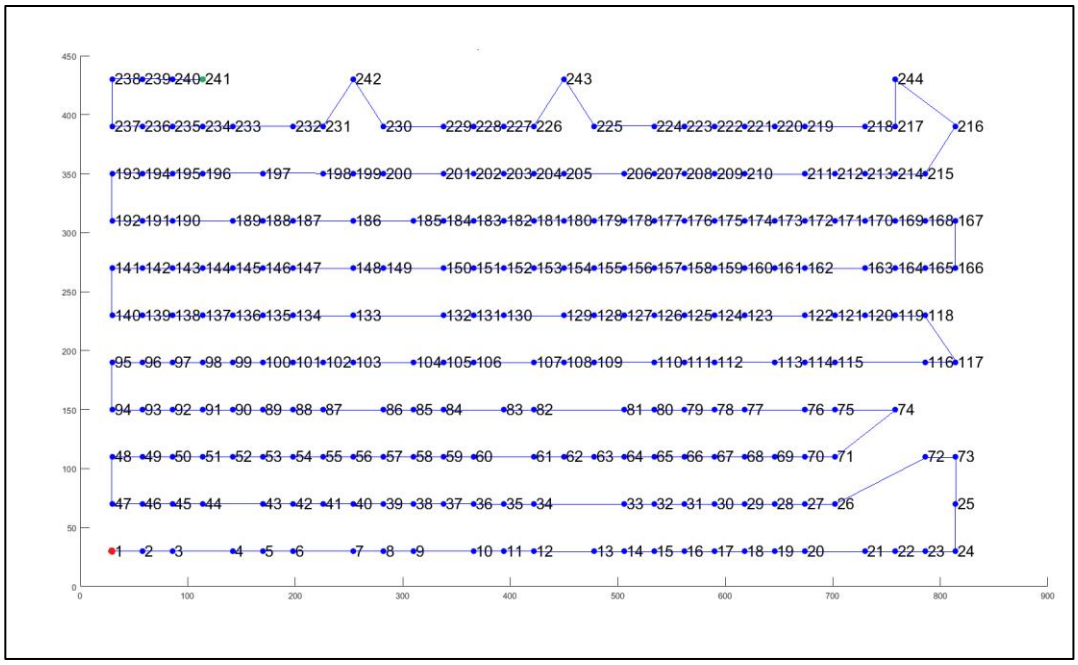
238 239 240 241 242 243 244
237 236 235 234 233 232 231 230 229 228 227 226 225 224 223 222 221 220 219 218 217 216
193 194 195 196 197 198 199 200 201 202 203 204 205 206 207 208 209 210 211 212 213 214 215
192 191 190 189 188 187 186 185 184 183 182 181 180 179 178 177 176 175 174 173 172 171 170 169 168 167
141 142 143 144 145 146 147 148 149 150 151 152 153 154 155 156 157 158 159 160 161 162 163 164 165 166
140 139 138 137 136 135 134 133 132 131 130 129 128 127 126 125 124 123 122 121 120 119 118
95 96 97 98 99 100 101 102 103 104 105 106 107 108 109 110 111 112 113 114 115 116 117
94 93 92 91 90 89 88 87 86 85 84 83 82 81 80 79 78 77 76 75 74
48 49 50 51 52 53 54 55 56 57 58 59 60 61 62 63 64 65 66 67 68 69 70 71 72 73
47 46 45 44 43 42 41 40 39 38 37 36 35 34 33 32 31 30 29 28 27 26 25
1 2 3 4 5 6 7 8 9 10 11 12 13 14 15 16 17 18 19 20 21 22 23 24

(d)

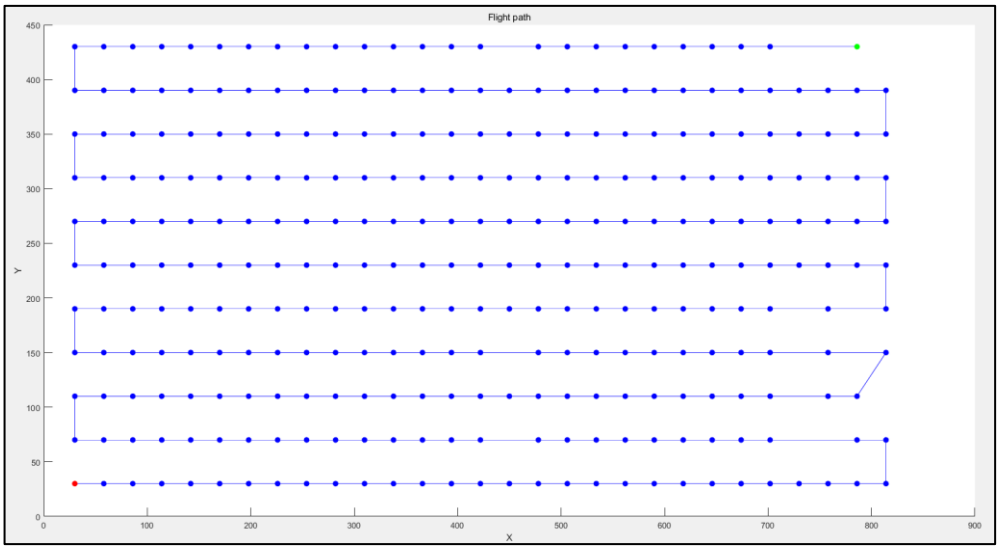

(e)

Figure4. 7 Optimal flight path (a. Scenario Ⅰ b. Scenario Ⅱ
c. Scenario Ⅲ d. Scenario Ⅳ e. Scenario Ⅴ)

5. DISCUSSION

In this chapter, the advantages and limitations of the methods used and different results under different scenarios are discussed.

5.1. Generation of synthetic terrain

The advantage of synthetic terrain is that the model is not constrained by data and can generate various DSMs to test the performance of the algorithm in different environments. This is exactly what the implemented algorithm needs. In this research, only several simple functional models were used to generate undulating terrain. Some more complex methods can be attempted for terrain construction in the future study, to make the generated synthetic DSM closer to reality.

5.2. Dense viewpoint network design

The generation of viewpoint network followed the traditional photogrammetry method, calculating the baseline length to determine the distance between two images and strip intervals for distance between strips. In the range of AOI, all the viewpoints in network were planned along the longer side in a sequence, and then planned strips in parallel. This research only considered the situation that AOI is rectangle. For other polygons that are not tested in this research, one suggested method to plan the flight strip is Cover Path Planning (CPP) algorithm.

All the viewpoints in network are nadir photography with the fixed exterior orientation parameters. In the future study, for those areas where the terrain is too undulating, oblique photography can be considered for photogrammetry if necessary.

5.3. Filter redundant images

The reduction in data size, which is also regarded as the redundancy rate of the data set, mainly depends on the set image overlap. For Scenario Ⅰ, Ⅱ and Ⅲ, which take 90% frontal overlap and 70% side overlap, the redundancy rate of data set is around 80% (80.1% for Scenario Ⅰ, 78.69% Scenario Ⅱ, and 76.25%for Scenario Ⅲ). And the redundancy rate shows a sharply decrease if the overlap percentage is 80% among the strip and 50% across the strip like Scenario Ⅳ, which is 23.51%. A higher overlap means a higher-density viewpoint network, resulting in the points in study area being repeatedly covered by the image multiple times, thus having such a high redundancy rate. In the real flight, for extreme terrain conditions, in order to avoid any loss of data quality caused by insufficient coverage, this high overlap sampling method is the most commonly used, which increase both data size and time cost for data processing. The algorithm developed by this research can filter out redundant images in this situation, and maximize the reduction of data size while ensuring coverage. The only difference between Scenario Ⅰ, Ⅱ and Ⅲ is that Scenario Ⅰ is flat terrain and the other two are undulating terrain. In the case of the same dense viewpoint network, the data size of Scenario Ⅱ and Ⅲ decreased by 78.69% and 76.25%, respectively, while Scenario Ⅰ was 80.1%. Due to the low flight height of UAV photogrammetry, the fluctuation of the terrain will affect the coverage area of a single image. Under the same percentage of overlap, images with a small coverage area are more likely to be retained to ensure full coverage of the

study area. As a result, the number of retained viewpoints in Scenario Ⅱ and Ⅲ is greater than that in Scenario Ⅰ, and the corresponding decrease in data size is smaller. By comparing the results of Scenario Ⅳ and Ⅴ, it could be found that the minimum visible times of points in study area "n" is also an important factor affecting the redundancy rate. As mentioned in Section 3.3, The value of "n" is used to check whether an image is redundant data. Therefore, the larger value of "n", the harder it is to define the image as redundant data. In the case where other parameters are the same, "n" increases from 3 to 4, the redundancy rate of the data set decreases from 23.51% to 4.39% (Scenario Ⅳ and Ⅴ).

The results of the algorithm at this stage have randomness, mainly related to the order of filtering. As shown in the Figure 5.1, point X is simultaneously observed by four images of 1, 2, 3, and 4. According to the principle that each point needs to be observed at least three times, the remaining three must be retained after any point is filtered out. The algorithm randomly selects images, and any point may be selected first. The difference in order when selecting points leads to randomness of results. This randomness has little effect on the number of viewpoints. Repeat this part of the algorithm using the same input parameters, the error is within ± 3.

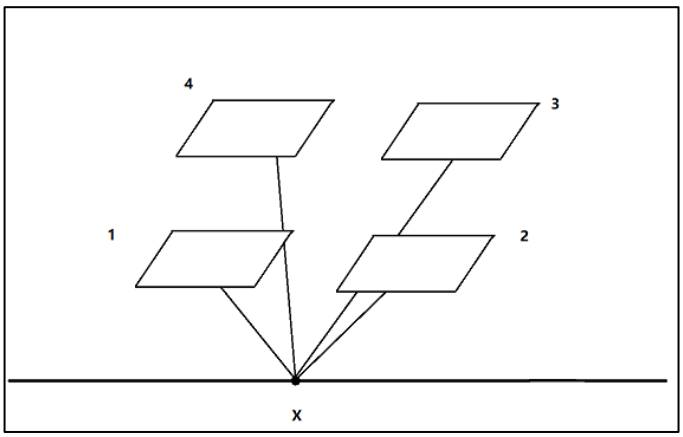

Figure5. 1 Randomness in filtering

Another reason for randomness result is the value "d" in algorithm (Figure 3.4), which represents the condition to terminate the filtering algorithm. The smaller the value of "d", the easier the algorithm terminates, resulting in some redundant images cannot be filtered out. But blindly increasing the "d" value will increase the running time of the algorithm. A suitable "d" value needs to be obtained through multiple tests. The initial "d" value set in this study is 100, the error is around ±10. Later, it was adjusted to 300 after repeated tests. Despite the increase in running time, the error is reduced to within ± 3. This can be regarded as a random result caused by the filtering order, because the error will not decrease when the "d" value is increased.

5.4. Flight path design

Compared with the conventional strip by strip flight path (called "S" path below), the optimization result of the flight time is not obvious. The maximum flight time reduction is around 7%, and the worst result is 0. The reason why the flight time optimization result is not obvious is mainly because the "S" path as the initial solution is the optimal flight path for photogrammetry without filtering redundant data. Considering that it is more difficult for a UAV to turn in the air than a straight flight, and an ordered image set helps to reduce the running time of bundle adjustment, so the general method to plan strips is parallel to the longest side of the study area, and then flying along "S" path to reduce the number of turns. In this study,

due to the redundant image filtering, there are many viewpoints removed in some strips. Flying these strips alone will unnecessarily increase the time cost. At this time, the algorithm is needed to search for a path with a shorter flight time. Since the algorithm originally takes the ordered "S" path as the input value, the improvement of the obtained optimization results is not obvious. There will even be situations where the optimal solution is the same as the initial solution like Scenario Ⅴ.

The flight path planning algorithm saves flight time and also brings some problems. As shown in Figure 5.2, there are some oblique strips in flight mission. Due to the exterior orientation parameters Omega (Ω), Phi (Φ) and Kappa (K) are defined as the fixed value in the research, the orientation of footprint will always follow the flight orientation, and it will cause oblique images. These inclinations caused by the change of flight orientation will increase the curvature of the strip and may cause inconsistent overlap. If the curvature is too large, it may cause missing of points and affect the data quality of photogrammetry.

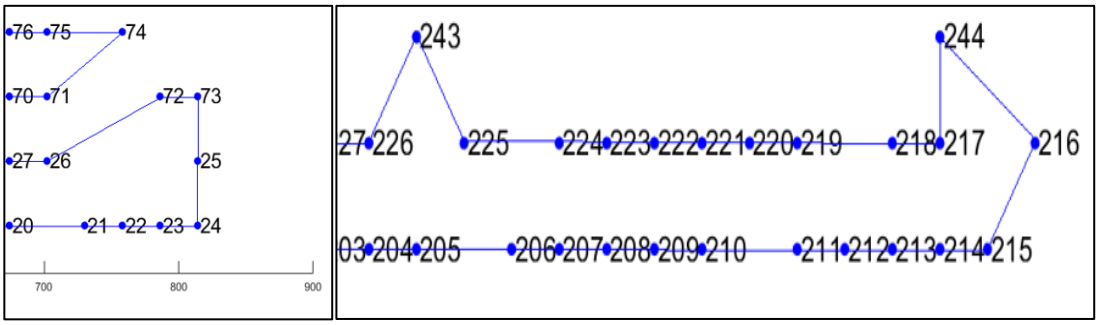

Figure5. 2 Part of oblique strips

6. CONCLUSION AND RECOMMENDATIONS

6.1. Conclusion

In this research, the algorithm was developed to calculate the positions of viewpoints for UAV that are required to acquire image set for mountainous area, using to get digital model products. Based on this, the synthetic DSM was generated and used as study area. From this DSM, the first thing to do is to design the dense viewpoint network. The input parameters of this step were not the undetermined camera interior parameters and GSD, but flight height, percentage of overlap and directly given angle α between the viewpoint and the edge of the image in the vertical direction. Calculating the baseline length and strip interval according to these input parameters to determine positions of all the viewpoints in network. Coverage check followed the principle that all the points on the DSM should be observed by at least "n" images (n equals 3 in the research, and have one scenario test the result if it is 4). Define that if an image in the dataset is deleted, the remaining images can still ensure that all points on the DSM can be observed by at least 3 images, then the deleted image is redundant data and can be removed, otherwise it will be reserved. Based on the definition of redundant image, using the method introduced in Section 3.3 to filter out all the redundant images. All viewpoints that capture the retained image are used as input data for path planning. The purpose of the algorithm in the optimal path planning stage is to use the Simulated Annealing Algorithm to find the path with the shortest flight time. In Section 3.4, this study improved the SAA algorithm to make it more suitable for UAV photogrammetry, including reducing the disturbance range of random solutions, no longer limiting the end point and most importantly, taking the flight time of conventional strip by strip path in photogrammetry as initial solution. And output result is the path of the drone with the shortest flight time. In the most extreme situation, this result is the initial solution.

The tests were performed on five scenarios with different terrain models and different input parameters. In general, the algorithm can provide the optimal results with minimum number of viewpoints that meet the complete coverage of the study area and the path with shortest flight time for all test scenarios. Except Scenario Ⅴ which take "n" value as 4 so that redundancy rate is only 4.39%, the reduction of data size is very large after optimizing by the algorithm, which is at least 23.51% and up to 80.1%. The decrease in data size mainly depends on percentage of overlap set when formulating photogrammetry missions. As for flight time, compared with the conventional strip by strip path, the optimization result of the flight time is not significantly improved, and the maximum reduction in flight time is 7.04%. The improvement of result is not obvious because the initial strip by strip path is originally an orderly and efficient solution.

The performance of the algorithm was good since it run successfully and got satisfactory results in redundant data filtering and flight path planning under all the scenarios created in this research. However, it still needs more tests to evaluate the quality of the results. The method using for dense viewpoints network design could be improved for those conditions that study areas are not just rectangular but other types of polygon as discussed in Section 5.1. And running time of redundant images filtering part need to be improved which cost quite a long time now. Additionally, it is impossible to quantify the errors caused by the change in flight orientation discussed in Section 5.3. It can only show that the simulated annealing algorithm does save flight time, but it will cause potential risk to the result.

6.2. Recommendations

This research only considered the situation that the study area is rectangular, and the synthesized terrain is mostly described by function curves. This simple DSM has no obvious significant for the large amount of algorithm testing work to be carried out next. And the rectangular study area makes the generation of dense viewpoint networks too simple. In fact, how to distribute the most reasonable strip in the study area is also a problem that can solved by the algorithm, which can be considered in future research.

The calculation method of the redundant data filtering method proposed by the author is too large, and the termination of the loop requires at least hundreds of consecutive runs without any images being deleted, resulting in a long running time. The CPU model used in this research is the Core i5-4200u dual-core processor (main frequency 1.6GHz, overclocking 2.6GHz), and the time for running a redundant data filtering algorithm is mostly concentrated in 40 to 50 minutes. Although the running time is closely related to the size of the "d" value (Figure 3.4), decreasing the "d" value will cause insufficient iterations, resulting in some redundant data cannot be filtered out. Therefore, in future research, if a larger DSM and more viewpoints are involved, the code needs to be improved to make it more streamlined to improve the efficiency of the algorithm.

Another limitation of the redundant data filtering part is the randomness of the results. Because the definition of redundant data is relative in itself. Any image in Figure 5.1 will be defined as redundant image, while the other three images will be retained. This error is inevitable

Because the flight path output by the algorithm has some inclined strips, and exterior orientation parameters Omega (Ω), Phi (Φ) and Kappa (K) are defined as the fixed value in the research. The images taken on these inclined strips are also inclined compared to the original strips. This curvature of the strip may bring potential risks to the data quality, like the different overlap, or the hole in digital model if it is worse. Because the entire process of this study uses simulated data, the accuracy of the data cannot be evaluated. Such a question can currently only be temporarily identified as a potential risk, and looking forward to the answers given by future research when testing algorithms in real flight. A probable way to solve this problem is that if there is any method to adjust the values of these three exterior parameters Omega (Ω), Phi (Φ) and Kappa (K) to ensure that the orientation of the footprint is always consistent with the original strip.

Expecting this algorithm will provide convincing results for UAV photogrammetry in realistic flight in the future!

LIST OF REFERENCES

Agatz, N., Bouman, P., & Schmidt, M. (2018). Optimization approaches for the traveling salesman problem with drone. *Transportation Science*, *52*(4), 965–981. https://doi.org/10.1287/trsc.2017.0791

Alsadik, B. (2014). Guided close range photogrammetry for 3D modelling of cultural heritage sites. In *ITC Dissertation*. https://doi.org/10.3990/1.9789036537933

Ambrosino, G., Ariola, M., Ciniglio, U., Corraro, F., De Lellis, E., & Pironti, A. (2009). Path generation and tracking in 3-D for UAVs. *IEEE Transactions on Control Systems Technology*, *17*(4), 980–988. https://doi.org/10.1109/TCST.2009.2014359

Baltsavias, E. P., Favey, E., Bauder, A., Bosch, H., & Pateraki, M. (2001). Digital Surface Modelling by Airborne Laser Scanning and Digital Photogrammetry for Glacier Monitoring. *The Photogrammetric Record*, *17*(98), 243–273. https://doi.org/10.1111/0031-868X.00182

Behnck, L. P., Doering, D., Pereira, C. E., & Rettberg, A. (2015). A modified simulated annealing algorithm for SUAVs path planning. *IFAC-PapersOnLine*, *28*(10), 63–68. https://doi.org/10.1016/j.ifacol.2015.08.109

Besada, J., Bergesio, L., Campaña, I., Vaquero-Melchor, D., López-Araquistain, J., Bernardos, A., & Casar, J. (2018). Drone Mission Definition and Implementation for Automated Infrastructure Inspection Using Airborne Sensors. *Sensors*, *18*(4), 1170. https://doi.org/10.3390/s18041170

Cabreira, T. M., Ferreira, P. R., Franco, C. Di, & Buttazzo, G. C. (2019). Grid-Based Coverage Path Planning With Minimum Energy Over Irregular-Shaped Areas With Uavs. *2019 International Conference on Unmanned Aircraft Systems (ICUAS)*, 758–767. https://doi.org/10.1109/ICUAS.2019.8797937

Cabreira, T. M., Franco, C. Di, Ferreira, P. R., & Buttazzo, G. C. (2018). Energy-Aware spiral coverage path planning for UAV photogrammetric applications. *IEEE Robotics and Automation Letters*, *3*(4), 3662–3668. https://doi.org/10.1109/LRA.2018.2854967

Caprara, A., Fischetti, M., & Toth, P. (1999). Heuristic method for the set covering problem. *Operations Research*, *47*(5), 730–743. https://doi.org/10.1287/opre.47.5.730

Castillo, O., Trujillo, L., & Melin, P. (2007). Multiple objective genetic algorithms for path-planning optimization in autonomous mobile robots. *Soft Computing*, *11*(3), 269–279. https://doi.org/10.1007/s00500-006-0068-4

Colomina, I., & Molina, P. (2014). Unmanned aerial systems for photogrammetry and remote sensing: A review. In *ISPRS Journal of Photogrammetry and Remote Sensing* (Vol. 92, pp. 79–97). Elsevier B.V. https://doi.org/10.1016/j.isprsjprs.2014.02.013

D'Oleire-Oltmanns, S., Marzolff, I., Peter, K., & Ries, J. (2012). Unmanned Aerial Vehicle (UAV) for Monitoring Soil Erosion in Morocco. *Remote Sensing*, *4*(11), 3390–3416. https://doi.org/10.3390/rs4113390

Dai, M., Tang, D., Giret, A., Salido, M. A., & Li, W. D. (2013). Energy-efficient scheduling for a flexible flow shop using an improved genetic-simulated annealing algorithm. *Robotics and Computer-Integrated Manufacturing*, *29*(5), 418–429. https://doi.org/10.1016/j.rcim.2013.04.001

Dandois, J. P., Olano, M., & Ellis, E. C. (2015). Optimal altitude, overlap, and weather conditions for computer vision uav estimates of forest structure. *Remote Sensing*, *7*(10), 13895–13920. https://doi.org/10.3390/rs71013895

Díaz-Varela, R., de la Rosa, R., León, L., & Zarco-Tejada, P. (2015). High-Resolution Airborne UAV Imagery to Assess Olive Tree Crown Parameters Using 3D Photo Reconstruction: Application in Breeding Trials. *Remote Sensing*, *7*(4), 4213–4232. https://doi.org/10.3390/rs70404213

Dueck, G., & Scheuer, T. (1990). Threshold accepting: A general purpose optimization algorithm appearing superior to simulated annealing. *Journal of Computational Physics*, *90*(1), 161–175. https://doi.org/10.1016/0021-9991(90)90201-B

Eisenbeiss, H. (2004). a Mini Unmanned Aerial Vehicle (Uav): System Overview and Image Acquisition. *Processing and Visualization Using High-Resolution Imagery*, 7. https://pdfs.semanticscholar.org/31e4/725e74bf623aeaf86782f52d9f140b2af153.pdf

Esposito, G., Mastrorocco, G., Salvini, R., Oliveti, M., & Starita, P. (2017). Application of UAV photogrammetry for the multi-temporal estimation of surface extent and volumetric excavation in the Sa Pigada Bianca open-pit mine, Sardinia, Italy. *Environmental Earth Sciences*, *76*(3), 1–16. https://doi.org/10.1007/s12665-017-6409-z

Eudossiana, V., & Planning, C. (2008). *Uav Application in Post – Seismic Environment*. *XL*(September 2013), 4–6.

Gruen, A., Zhang, Z., & Eisenbeiss, H. (2012). UAV PHOTOGRAMMETRY IN REMOTE AREAS – 3D MODELING OF DRAPHAM DZONG BHUTAN. *ISPRS - International Archives of the Photogrammetry, Remote Sensing and Spatial Information Sciences*, *XXXIX-B1*, 375–379. https://doi.org/10.5194/isprsarchives-xxxix-b1-375-2012

Gülch, E. (2012). *PHOTOGRAMMETRIC MEASUREMENTS IN FIXED WING UAV IMAGERY*.

Gupta, S. G., Ghonge, M., & Jawandhiya, P. M. (2019). Review of Unmanned Aircraft System (UAS). *SSRN Electronic Journal*, *April*. https://doi.org/10.2139/ssrn.3451039

Ham, Y., Han, K. K., Lin, J. J., & Golparvar-Fard, M. (2016). Visual monitoring of civil infrastructure systems via camera-equipped Unmanned Aerial Vehicles (UAVs): a review of related works. In *Visualization in Engineering* (Vol. 4, Issue 1). Springer. https://doi.org/10.1186/s40327-015-0029-z

Harwin, S., & Lucieer, A. (2012). Assessing the Accuracy of Georeferenced Point Clouds Produced via Multi-View Stereopsis from Unmanned Aerial Vehicle (UAV) Imagery. *Remote Sensing*, *4*(6), 1573–1599. https://doi.org/10.3390/rs4061573

Heintz, F., Rudol, P., & Doherty, P. (2007). From images to traffic behavior - A UAV tracking and monitoring application. *FUSION 2007 - 2007 10th International Conference on Information Fusion*. https://doi.org/10.1109/ICIF.2007.4408103

Hu, X., Zhenqi, H., & Jianyong, Z. (2017). The status and prospect of UAV remote sensing in mine monitoring and land reclamation. *CHINA MINING MAGAZINE*, *26*(6), 71–78.

Keller, J., Thakur, D., Likhachev, M., Gallier, J., & Kumar, V. (2017). Coordinated path planning for fixed-wing UAS conducting persistent surveillance missions. *IEEE Transactions on Automation Science and Engineering*, *14*(1), 17–24. https://doi.org/10.1109/TASE.2016.2623642

Kirkpatrick, S., & Selman, B. (1994). Critical behavior in the satisfiability of random Boolean expressions. *Science*, *264*(5163), 1297–1301. https://doi.org/10.1126/science.264.5163.1297

Li, Y., Chen, H., Joo Er, M., & Wang, X. (2011). Coverage path planning for UAVs based on enhanced exact cellular decomposition method. *Mechatronics*, *21*(5), 876–885. https://doi.org/10.1016/j.mechatronics.2010.10.009

Lin, S., & Kernighan, B. W. (1973). EFFECTIVE HEURISTIC ALGORITHM FOR THE TRAVELING-SALESMAN PROBLEM. *Operations Research*, *21*(2), 498–516. https://doi.org/10.1287/opre.21.2.498

Linder, W. (2009). *Digital photogrammetry*. https://doi.org/10.4324/9780203305959

Liu, X., Liu, Y., Zhang, N., Wu, W., & Liu, A. (2019). Optimizing trajectory of unmanned aerial vehicles for efficient data acquisition: A matrix completion approach. *IEEE Internet of Things Journal*, *6*(2), 1829–1840. https://doi.org/10.1109/JIOT.2019.2894257

McKendall, A. R., Shang, J., & Kuppusamy, S. (2006). Simulated annealing heuristics for the dynamic facility layout problem. *Computers and Operations Research*, *33*(8), 2431–2444. https://doi.org/10.1016/j.cor.2005.02.021

Meng, H., & Xin, G. (2010). UAV route planning based on the genetic simulated annealing algorithm. *2010 IEEE International Conference on Mechatronics and Automation, ICMA 2010*, 788–793. https://doi.org/10.1109/ICMA.2010.5589035

Metropolis, N., Rosenbluth, A. W., Rosenbluth, M. N., Teller, A. H., & Teller, E. (1953). Equation of state calculations by fast computing machines. *The Journal of Chemical Physics*, *21*(6), 1087–1092. https://doi.org/10.1063/1.1699114

Morbidi, F., Cano, R., & Lara, D. (2016). Minimum-energy path generation for a quadrotor UAV. *Proceedings - IEEE International Conference on Robotics and Automation*, *2016-June*, 1492–1498. https://doi.org/10.1109/ICRA.2016.7487285

Ólafsson, S. (2006). Metaheuristics. *Handbooks in Operations Research and Management Science*, *13*(C), 633–654. https://doi.org/10.1016/S0927-0507(06)13021-2

Peter, K. D., d'Oleire-Oltmanns, S., Ries, J. B., Marzolff, I., & Ait Hssaine, A. (2014). Soil erosion in gully catchments affected by land-levelling measures in the Souss Basin, Morocco, analysed by rainfall simulation and UAV remote sensing data. *Catena*, *113*, 24–40. https://doi.org/10.1016/j.catena.2013.09.004

Phung, M. D., Quach, C. H., Dinh, T. H., & Ha, Q. (2017). Enhanced discrete particle swarm optimization path planning for UAV vision-based surface inspection. *Automation in Construction*, *81*, 25–33. https://doi.org/10.1016/j.autcon.2017.04.013

Piras, M., Taddia, G., Forno, M. G., Gattiglio, M., Aicardi, I., Dabove, P., Russo, S. Lo, & Lingua, A. (2017a). Detailed geological mapping in mountain areas using an unmanned aerial vehicle: application to the Rodoretto Valley, NW Italian Alps. *Geomatics, Natural Hazards and Risk*, *8*(1), 137–149. https://doi.org/10.1080/19475705.2016.1225228

Piras, M., Taddia, G., Forno, M. G., Gattiglio, M., Aicardi, I., Dabove, P., Russo, S. Lo, & Lingua, A. (2017b). Detailed geological mapping in mountain areas using an unmanned aerial vehicle: application to the Rodoretto Valley, NW Italian Alps. *Geomatics, Natural Hazards and Risk*, *8*(1), 137–149. https://doi.org/10.1080/19475705.2016.1225228

Qu, Y. H., Pan, Q., & Yan, J. G. (2005a). Flight path planning of UAV based on heuristically search and genetic algorithms. *IECON Proceedings (Industrial Electronics Conference)*, *2005*, 45–49. https://doi.org/10.1109/IECON.2005.1568876

Qu, Y. H., Pan, Q., & Yan, J. G. (2005b). Flight path planning of UAV based on heuristically search and genetic algorithms. *IECON Proceedings (Industrial Electronics Conference)*, *2005*, 45–49. https://doi.org/10.1109/IECON.2005.1568876

Ruggles, S., Clark, J., Franke, K. W., Wolfe, D., Reimschiissel, B., Martin, R. A., Okeson, T. J., & Hedengren, J. D. (2016). Comparison of SfM computer vision point clouds of a landslide derived from multiple small UAV platforms and sensors to a TLS-based model. *Journal of Unmanned Vehicle Systems*, *4*(4), 246–265. https://doi.org/10.1139/juvs-2015-0043

Shunhai, J., & Yao, L. (2014). The Application of UAV Remote Sensing Technologyin Land Consolidation Construction Monitoring. *Modern Surveying and Mapping*, *37*(3), 48–50.

Sislak, D., Sislak, D., Volk, P., Volk, P., Pechoucek, M., & Pechoucek, M. (2009). Flight Trajectory Path Planning. *2009 ICAPS Scheduling and Planning Applications WoRKshop (SPARK)*, 76–83.

Stocker，C, Nex, F., Koeva, M., & Gerke, M. (2019). *UAV-BASED CADASTRAL MAPPING : AN ASSESSMENT OF THE IMPACT OF FLIGHT PARAMETERS AND GROUND TRUTH MEASUREMENTS ON THE ABSOLUTE ACCURACY OF DERIVED ORTHOIMAGES*. *XLII*(June), 10–14.

Stöcker, C., Eltner, A., & Karrasch, P. (2015). Measuring gullies by synergetic application of UAV and close range photogrammetry - A case study from Andalusia, Spain. *Catena*, *132*, 1–11. https://doi.org/10.1016/j.catena.2015.04.004

Sujit, P. B., Hudzietz, B. P., & Saripalli, S. (2013). Route planning for angle constrained terrain mapping using an unmanned aerial vehicle. *Journal of Intelligent and Robotic Systems: Theory and Applications*, *69*(1–4), 273–283. https://doi.org/10.1007/s10846-012-9729-y

Tsardoulias, E. G., Iliakopoulou, A., Kargakos, A., & Petrou, L. (2016). A Review of Global Path Planning Methods for Occupancy Grid Maps Regardless of Obstacle Density. *Journal of Intelligent and Robotic Systems: Theory and Applications*, *84*(1–4), 829–858. https://doi.org/10.1007/s10846-016-0362-z

Turker, T., Sahingoz, O. K., & Yilmaz, G. (2015). 2D path planning for UAVs in radar threatening environment using simulated annealing algorithm. *2015 International Conference on Unmanned Aircraft Systems, ICUAS 2015*, 56–61. https://doi.org/10.1109/ICUAS.2015.7152275

Turker, T., Yilmaz, G., & Sahingoz, O. K. (2016). GPU-accelerated flight route planning for multi-UAV systems using simulated annealing. *Lecture Notes in Computer Science (Including Subseries Lecture Notes in Artificial Intelligence and Lecture Notes in Bioinformatics)*, *9883 LNAI*, 279–288. https://doi.org/10.1007/978-3-319-44748-3_27

Wallace, L., Lucieer, A., Watson, C., & Turner, D. (2012). Development of a UAV-LiDAR system with application to forest inventory. *Remote Sensing*, *4*(6), 1519–1543. https://doi.org/10.3390/rs4061519

Wang, F., Cui, J.-Q., Chen, B.-M., & Lee, T. H. (2013). A Comprehensive UAV Indoor Navigation System Based on Vision Optical Flow and Laser FastSLAM. *Acta Automatica Sinica*, *39*(11), 1889–1899. https://doi.org/10.1016/S1874-1029(13)60080-4

Yang, G., & Kapila, V. (2002). Optimal path planning for unmanned air vehicles with kinematic and tactical constraints. *Proceedings of the IEEE Conference on Decision and Control*, *2*, 1301–1306. https://doi.org/10.1109/cdc.2002.1184695

Zhang, C., Zhen, Z., Wang, D., & Li, M. (2010). UAV path planning method based on ant colony optimization. *2010 Chinese Control and Decision Conference, CCDC 2010*, 3790–3792. https://doi.org/10.1109/CCDC.2010.5498477

Zhang, Z., Schwartz, S., Wagner, L., & Miller, W. (2000). A greedy algorithm for aligning DNA sequences. In *Journal of Computational Biology* (Vol. 7, Issues 1–2, pp. 203–214). Mary Ann Liebert, Inc. . https://doi.org/10.1089/10665270050081478